ELSEVIER

Journal of Chromatography A, 698 (1995) 55–87

JOURNAL OF CHROMATOGRAPHY A

Review

Biologist's perspective on analytical imaging systems as applied to protein gel electrophoresis

Wayne F. Patton

Microvascular Research Division, Biological Sciences Center and the Center for Photonics Research, Boston University, 5 Cummington Street, Boston, MA 02115 USA

Abstract

High-resolution two-dimensional polyacrylamide gel electrophoresis entails the separation of proteins in the first dimension according to their charge and in the second dimension according to their relative mobility (R_F). The technique is capable of simultaneously resolving thousands of polypeptides as a constellation pattern of spots. Ultimately, the level of success in the analysis of such protein patterns depends upon the quality of the protein separation, the sensitivity of the procedures used to visualize the proteins, and the resolution of the image capture device used for quantitative measurements. A number of analytical imaging systems that combine machine vision, digital image processing and data processing are available for interpretation of the complex patterns generated by the technique. The most common input devices for obtaining images of electrophoresis gels are charge-coupled device camera systems and document scanners. Gaussian and median filters are often used to reduce noise in the digitized gel images. After image acquisition, spot boundaries are detected, the amount of protein in each spot is established, and the coordinates of each spot are determined. The images are then linked together into a gel database and relevant spots are located by user specified queries. The computer excels at providing unbiased detection of quantitative differences in hundreds or even thousands of proteins across large numbers of gels.

Contents

0021-9673/95/$29.00
SSDI 0021-9673(94)00987-2

1. Introduction

It is my intention to provide a practitioner's view of electrophoretic imaging technology. Like the vast majority of individuals utilizing two-dimensional (2D) gel electrophoresis in their research, I have never written my own computer program for gel analysis. I feel that in the past, too many reviews on gel image analysis have been burdened with obtuse computer jargon as well as endless pictures of windows and menus from specific programs. On the other hand, few direct comparisons have been made between different visualization techniques, input devices, image processing strategies, and spot finding/quantification methods. I hope to provide some comparisons based upon instrumentation I have had experience with and provide guidance with respect to strategies used to solve day-to-day image analysis problems in my laboratory. I hope to keep the review focused upon addressing the real needs of biological scientists.

1.1. Why computer analysis of gels is necessary

The biological sciences have not relied as heavily upon mathematics as other fields such as physics, physical chemistry or computer sciences. Though word processors, spreadsheets and graphics illustration programs have been assimilated into the biologist's culture, there is still a genuine distrust of computers in particular and a phobia of mathematics in general among many in the field. It is not uncommon to encounter biologists that are completely opposed to the concept of quantitative image analysis of gels. They insist that they can determine one-dimensional (1D) peak centroids better than any mathematical morphology algorithm (not necessarily in those words), and that they can find differences between 2D gel patterns better than any computerized gel database. They dismiss the capability of accurately detecting small quantitative changes between proteins as being inconsequential. "If the change is not readily apparent to me by eye, then it is unimportant".

Fundamentally, the role of human vision is quite different from that of the computerized densitometer. The human eye transforms 2D data into a description of the three-dimensional world [1]. Many brightness optical illusions are based upon the psychology of the human eye–brain combination [2]. As a detector, the human eye is subject to low-level processes such as the lateral inhibition of cells in one region of the retina by cells in adjacent regions. Analogous problems occur in some inanimate visual systems. As an example, charge-coupled device (CCD) cameras are subject to "bloom" around bright regions in an image, causing a spread of excessive output over a wider than true area. More importantly though, the human brain, firmly grounded in interpretation of phenomena in a three-dimensional world, adds another layer of complexity to the analysis, since the visual system also automatically attempts to estimate the reflectances of surfaces and this lightness perception inevitably influences the judgment of brightness [1,2]. As a result, modest changes in geometry substantially alter brightness perception.

Despite its limitations, the human eye–brain combination is a powerful tool for extracting information from electrophoresis gels. All gels in my laboratory are visually evaluated prior to any computerized analysis. At the very least, this visual inspection is important in determining whether the particular electrophoresis run met laboratory quality standards. For many projects, visual inspection is sufficient to answer the scientific question posed. It is fairly simple to determine by eye whether or not an inducer of myeloid cell differentiation caused an increase in actin expression. Computerized gel analysis is utilized simply to determine how much the actin is up-regulated by the inducing agent. Similarly, the biologist experienced in cytoskeletal profiles can determine whether or not a particular sarcoma has specific intermediate filaments in it by a simple cursory glance of the 2D gel. In such projects, computerized gel analysis serves as an adjunct technology, providing a convenient method to accurately determine molecular mass (M_r) and isoelectric point (pI) values for the proteins. A great majority of biological research is performed at this level, even in my laboratory.

Image flickering procedures have been developed to augment visual inspection of gels [3,4]. In their simplest implementation, the two gels are placed on projectors and the images are combined on a digitizing platform. The lights on the two projectors are switched on and off, out of phase, so that the positions of the common spots remain unchanged, while those that are spatially displaced appear to jump from one position to another and those absent on one gel turn on and off periodically. Clearly, visual inspection of gels is simple and cost effective. It is suitable for initial evaluation of experiments but does not provide the minimum necessary parameters required for construction of gel databases (protein amount, M_r and pI). Protein spots can be quantified individually by cutting out radiolabeled proteins and determining the radioactivity in each spot using a scintillation or γ counter. Dye-stained gels can also be processed by cutting out the individual spots, eluting the dye and measuring the concentration spectrophotometrically. These procedures destroy

the gel and require a considerable amount of book keeping to organize the data.

While the human eye–brain combination can detect qualitative differences in a particular spot present on a reference and study gel, the computer excels at providing reproducible, unbiased detection of quantitative differences in hundreds or even thousands of proteins across large numbers of gels. Spot boundaries are demarcated in an identical manner for all polypeptides on all gels being studied. The computer assists in organizing the vast amounts of data into a readily interpretable form.

1.1.1. Kinetic analysis and dose response

With appropriate equipment, quantitative image analysis can provide extraordinary research capabilities to a project. Utilizing a CCD camera, for instance, allows one to perform dynamic, real-time kinetic analyses of enzyme activities without purification of the specific isozymes [5]. As an example, in conventional enzymology studies phosphatases can be evaluated spectrophotometrically utilizing substrates such as *p*-nitrophenyl phosphate. Hydrolysis of the phosphate ester releases the chromogen, *p*-nitrophenol which can be detected by its absorbance at 430 nm. When such experiments are performed on complex cell lysates, an average phosphatase response is measured resulting from the activities of several isozymes in the sample. If non-denaturing 1D or 2D electrophoresis is performed and enzymes are detected in the gel or on electroblotted membranes using appropriate substrates (i.e. 4-methylumbelliferyl phosphate or α-naphthyl phosphate coupled with fast blue BB), multiple phosphatase isozymes can be monitored simultaneously. Multiple gels can be processed with differing amounts of substrates and inhibitors added. Standard enzyme parameters such as K_m, K_i, V_{max} and substrate preference can thus be established for each isozyme in the sample [5,6]. Quantitative zymographic determination of picogram amounts of active and latent forms of matrix metalloproteases can be achieved readily by gel image analysis [7]. Similarly, dose–response curves for several components of a complex mixture of proteins can be determined by quantitative image analysis of radiolabeled or stained proteins. The co-regulation of several polypeptides in a complex sample can thus easily be established [8]. This approach has been utilized effectively to identify transformation-sensitive polypeptides in rat and human cells [9,10].

A computerized imaging system is also a convenient, albeit expensive, tool for the assay of protein amount [11]. While an investigator would not buy a system expressly for the purposes of performing protein assays, it is reasonable to extend the usefulness of an instrument already available for gel analysis. In my laboratory, standard and test proteins are spotted onto nitrocellulose membranes, then stained utilizing colloidal gold or preferably ferric chelate stains, and quantified by a CCD camera system. The recently developed ferric chelate stains are readily reversible, are completely compatible with immunoblotting and microsequencing techniques and display a wider dynamic range than colloidal gold stains [12]. While standard protein assays such as the Folin–phenol method of Lowry require 10 μg of protein, the colloidal gold and ferric chelate methods can detect as little as 1.25 ng of protein [11–13]. Membrane-based protein assays allow accurate protein quantitation utilizing only a microliter of sample [11,12].

1.1.2. Diagnosis

Members of the Hochstrasser laboratory have been major proponents of the use of 2D gel electrophoresis as a diagnostic tool [14–16]. Their goal has been to establish classification programs that aid the physician in finding disease-associated proteins as well as artificial intelligence programs that automatically propose diagnoses. In a recent study, heuristic clustering techniques were able to differentiate between liver biopsy patterns from control rats and rats suffering from cirrhosis [15]. The techniques were also successful in automatically differentiating between lung epidermoid carcinomas, rectal adenocarcinomas and lymphomas but failed to differentiate between pleural and ascites fluid [15]. Pleural and ascites fluid are difficult for the trained expert to distinguish between by eye.

Utilizing neural network procedures, 71–74% of the physiological fluid patterns were correctly classified [15]. Thus, while not yet a reality, computerized, diagnostic 2D gel electrophoresis appears to be quite a feasible possibility.

An alternative strategy for utilizing 2D gel electrophoresis as a diagnostic tool acquiesces to the fact that the technique is not suitable as a routine clinical test since it is a low-throughput and labor-intensive method [17]. Instead, the procedure is envisioned as a tool for exploratory analysis. Once potential biomarkers for a particular disease are identified by image analysis, antisera are generated to relevant polypeptides and used in high-throughput immunoassays for screening larger sample sets. In a study of occupational exposure to cadmium, a group of low-M_r, acidic proteins were identified in urine that indicate toxicity effects associated with the proximal tubule [17].

1.1.3. Subtractive library

I have found the "subtractive library" approach to 2D gel electrophoresis of great value in the study of phenotypic differences between ontogenetically related cell types [18,19]. This is perhaps the most widely used and intuitive approach to 2D gel analysis. The large number of polypeptides shared by both the reference sample and the study sample are ignored and only differences between the samples are further evaluated. This qualitative analysis can be performed manually but is much more easily performed utilizing a computer. When performed by eye, the reference and study gel are evaluated, spot by spot, using a light box. Differences are then confirmed by evaluating other study and reference gels for the same changes. When performed by computer, several reference and study gels are linked together in a database. The database is then queried: "Show me spots that appear on at least two gels but are not found on all gels in the experiment". The constraint that the spot must appear in at least two gels removes any spurious spot-like features that may be present on a particular gel (bubbles, tears). Once such a database is constructed, it is a simple matter to relax the constraints and ask for spots that differ quantitatively (i.e. by 3-fold or more) between the reference and study gels.

1.2. Optimizing gels for image analysis

One critical feature often ignored in discussions of computerized gel analysis is the importance of generating reproducible, high-quality electrophoretic patterns [20]. Even low-end analytical imaging systems can provide adequate quantitative data when presented with a high-quality gel, containing well separated spots. A great deal of effort has been expended in programming high-end gel analysis systems to be able to remove tears in the gels and to correct for local distortions due to stretching of isoelectric focusing (IEF) gels, uneven heating of slab gels or electrical leaks from poorly sealed gel spacers. Nevertheless, it is prudent to avoid such artifacts when ever possible as "patched up" gels are never of equivalent quality to gels not requiring computer generated repairs. Similarly, while many computerized systems provide automated methods for the Gaussian deconvolution of overlapping spots, better quantitative results are obtained if the overlap of spots is minimized by running larger gels. To obtain the maximum information from a complex protein mixture we have found it critical to use a large format gel system [20].

Recently, we introduced a technique for reduction of pattern distortion due to stretching of the IEF gel [20]. The technique utilizes a 1 mm capillary tube with a 0.08 mm thread incorporated along its length prior to polymerization of the gel matrix. The thread acts as a mechanical support for the IEF gel. We also introduced an improved second-dimension matrix resistant to tearing during handling (Duracryl, Millipore) [21]. The matrix is based on acrylamide–N,N′-bisacrylamide but also contains synthetic polymers that double the tensile strength of the gel relative to conventional gels. The concept is similar to that employed in the building industry, where steel-reinforcing rods are added to strengthen concrete. Alternatively, an agarose-based cross-linker (AcrylAide, FMC BioProducts) can be utilized in both dimensions of the

gel to enhance mechanical strength [17]. Mechanical stabilization of the IEF and sodium dodecyl sulfate (SDS)–polyacrylamide gel electrophoresis (PAGE) gel matrices reduces damage due to manual handling of the media during post-electrophoretic processing procedures such as staining and drying. Improved computerized 2D gel analysis can be achieved simply by increasing gel resolving power, minimizing gel artifacts and enhancing gel to gel reproducibility.

1.2.1. Quantitative silver staining of gels

Silver staining allows detection of low nanogram amounts of protein. The prevailing belief amongst practitioners of electrophoresis is that silver staining cannot be used for quantitative studies. Often, Coomassie Brilliant Blue staining is utilized for quantitative analysis instead, even though it is at least 20-fold less sensitive than silver staining. Quantitative studies of Coomassie Brilliant Blue-stained proteins are not without their own perils, as secondary dye-binding and dye–dye interactions may generate metachromatic artifacts that interfere with analysis [22]. It is important to remember that there are numerous silver-staining procedures based upon radically different chemistries and that the stoichiometric or non-stoichiometric behavior of the silver stain depends upon which method is utilized. The two major families of silver stain utilized in protein electrophoresis are the silver diammine and silver nitrate methods [22]. A number of high-quality diammine and nitrate-based staining procedures were recently compared to one another with respect to sensitivity, and applicability to 1D and 2D electrophoresis [23]. Many of the newer staining procedures are far superior to the classical techniques developed in the early 1980s (reviewed in [23]). These older methods often generate polychromatic spots varying in hue from red to black. Red-yellow backgrounds rapidly appear in the developing solution when utilizing the older methods which prohibits further development and reduces sensitivity. The newer methods consistently maintain clear backgrounds, some for as long as 1–2 h of development [23]. Several diammine- and nitrate-based staining protocols are capable of detecting as little as 125 to 300 pg/mm^2 of protein [23]. Polypeptides stained by silver diammine procedures are difficult to quantify, however [24]. Five different staining behaviors were observed in a real-time analysis of the slopes of integrated absorbance (IA) as a function of time for 18 marker polypeptides from 2D gels [24]. Thus, without a priori information concerning the staining properties of each and every spot in the pattern, there is no simple way to predict the amount of protein present in a spot from its IA using the particular diammine procedure studied. We decided to evaluate the stoichiometric properties of the silver nitrate procedure developed by Rabilloud's laboratory and routinely used in our laboratory (Table 2, 3rd column, in Ref. [23]). A real-time analysis of 100 polypeptides was performed from 2D gels during silver-stain development. Representative quantitative data from six proteins in the study are shown in Fig. 1. Images were obtained every minute for a 10-min period and every 5 min for an additional 10 min using a CCD camera system. Unlike the diammine procedure, the nitrate procedure provided a consistent linear response from 2 min through 10 min development time ($r = 0.960 \pm 0.041$, $n = 100$). Many spots (70%) then exhibited a saturation response by 20 min development time. This saturation response is similar to the saturation response observed during autoradiography and thus does not invalidate the silver-stain procedure for quantitative analysis. A calibration strip should be included with the gel to be stained as previously suggested for quantitative autoradiography [25]. With the nitrate-based silver stain, it is possible to achieve quantitative results by developing gels for a defined length of time. Very-low-abundance proteins can be detected by extending the development time to an hour or two but the gel is then only suitable for qualitative studies. It should be remembered that, even with optimal development times, the total integrated intensity of a silver- or Coomassie Brilliant Blue-stained spot can only be regarded as semi-quantitative since the stains do not rigorously obey Beer–Lambert's law [26]. This is not a serious problem, since the biologist is generally interested in

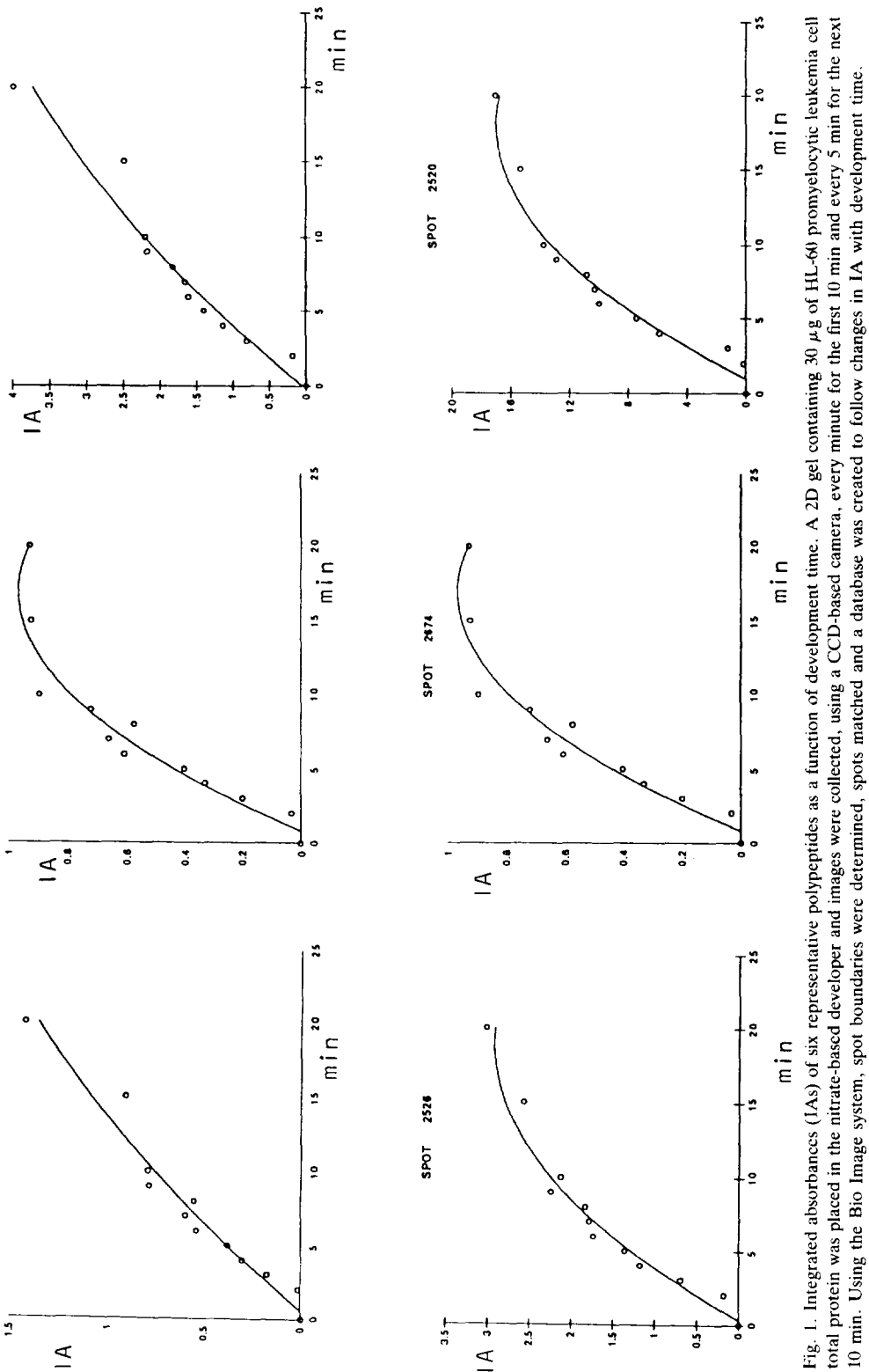

Fig. 1. Integrated absorbances (IAs) of six representative polypeptides as a function of development time. A 2D gel containing 30 μg of HL-60 promyelocytic leukemia cell total protein was placed in the nitrate-based developer and images were collected, using a CCD-based camera, every minute for the first 10 min and every 5 min for the next 10 min. Using the Bio Image system, spot boundaries were determined, spots matched and a database was created to follow changes in IA with development time.

comparably large differences in relative intensities.

1.3. Fractionation of lysates to improve detection

Especially with the advent of ultrasensitive silver-staining procedures, it is often necessary to fractionate samples prior to performing electrophoretic analysis. Utilizing large-format 2D gels allows one to resolve 1500 to 3000 polypeptides in a complex cell lysate. Often, however, the low-abundance polypeptides are obscured by the high abundance ones. Recently, we examined changes in stationary and proliferating rat aortic smooth muscle cells by quantitative 2D gel electrophoresis [27,28]. About a dozen changes were revealed by computerized analysis of the gels. Internal amino acid sequencing revealed that many of the proteins were components of the protein synthesis and folding machinery (an elongation factor, heat shock proteins and disulfide isomerases). All of the proteins identified in our study by co-electrophoresis and protein microsequencing were among the 763 proteins previously identified in the human keratinocyte 2D database [10,29]. It is often the lowest abundance polypeptides that are of the greatest interest to many researchers, who feel it is more important to discover brand new, uncharacterized proteins than to understand ones that are already present in on-line protein databases. Two-dimensional gel electrophoresis is more likely to provide data on the high copy number components of a fraction. This problem is not unique to the technique, however. Recently, an analysis of mRNA from proliferating and quiescent smooth muscle cells was performed [30]. The differential cDNA screening experiments revealed changes in the highest abundance cytoskeletal gene products such as actin, vinculin, tropomyosin and calmodulin. To obtain usable information on low abundance species, it is often necessary to fractionate samples prior to electrophoretic analysis.

1.3.1. Subcellular fractionation

Conventional methods of subcellular fractionation such as differential centrifugation and ion-exchange chromatography are compatible with 2D electrophoresis, providing that care is taken to remove salts from the sample prior to analysis. Differential detergent fractionation of cells is an effective means of simplifying electrophoretic patterns as well. Triton X-114 detergent extraction is a widely used method for separating cells into three components; insoluble cytoskeleton, integral membrane, and soluble cytosol fractions [31]. A more elaborate detergent fractionation procedure is reported to separate cells into cytosolic, membrane–organelle, nuclear membrane and cytoskeletal–matrix fractions [32]. The appeal of these extraction protocols is that the detergent buffers are all fully compatible with equilibrium and non-equilibrium 2D gel electrophoretic techniques.

1.3.2. Metal affinity and triazine dye fractionation

Immobilized metal affinity chromatography involves fractionation of proteins by metal ions (e.g. Zn^{2+}, Ni^{2+} and Cu^{2+}) that have been immobilized to a chelating matrix containing iminodiacetic acid side chains [33]. The procedure is fully compatible with 2D gel electrophoresis. Protein binding is mediated by the presence of surface histidyl, cysteinyl or tryptophyl moieties on the protein. Dye ligand chromatography has been shown to be an efficient means of simplifying 2D gel patterns, as well [34]. Protein fractionation by dye ligand chromatography is thought to result from a combination of ion-exchange, diffusion–exclusion, pseudo-ligand affinity and hydrophobic interactions [35]. As an example, enzymes that bind ATP, NAD and some other purine nucleotides have been found to be absorbed to Blue A-Sepharose columns [34]. Both binding and non-binding fractions are readily evaluated by 2D gel electrophoresis [33,34]. Chromatographic prefractionation of protein samples by either procedure increases resolution by two-fold. This may be due to the increase in separation area from a single gel (total lysate) to two gels (bound and unbound fractions) or may be due to concentration of the less abundant polypeptides by the column.

2. Image capture (input devices compared)

Traditional, 1D line-scanning densitometers have largely been superseded by instruments that collect data in two dimensions. While 1D gels can be analyzed using a 1D peak volume integration approach, whole band analysis is preferable as protein bands generated by 1D gel electrophoresis are in fact dumbbell shaped. Individual spots from 2D gels have also been analyzed on 1D line-scanning densitometers [36]. Selected spots are scanned in the horizontal and vertical direction. The densitometric response is then related to the volume of an ellipsoid. After establishing a baseline and peak height, proteins of known amount are scanned in the x and y directions. Ellipsoid volume integrals are calculated and plotted against the amount of protein to form the standard curve. The amount of protein in the unknown spot is then read directly from the standard curve. To perform such an analysis on more than a few proteins from a single gel quickly becomes a Herculean feat.

An entire review article could be devoted to the application of image capture devices to electrophoresis. A well written review on this very subject was recently published and should be consulted by those particularly interested in this aspect of analytical electrophoretic imaging [37]. The two most common types of input devices for gel imaging are scanner- and camera-based systems. Additionally, phosphor storage imaging technology has been adopted by many of the larger institutions for analysis of radioactively labeled material. An alternative technology for spatial quantitation of radionucleotides is the multichannel array detector. Methods for directly imaging unstained gels have been developed as well but are of limited utility.

2.1. Charge-coupled device cameras

The CCD chip is a silicon array imaging device that detects light intensity [38]. The CCD camera is used to replace conventional cameras that utilize photographic film and depends on the same optical design as its predecessors. Instead of having a piece of film in the focal plane of the lens, there is a transistorized light sensor on an integrated circuit, the CCD chip. The silicon crystal is an array of atoms whose bonds can be broken by absorbing light of various wavelengths. The breaking of these bonds causes electrons to be released but maintained in that localized region of the chip until they are collected and read by the computer. The electrically charged regions thus generated are translated by an analog-to-digital (A/D) converter into digital information. When a polyacrylamide gel is digitized by a CCD camera and the image is stored onto the hard disk of a computer, image intensities are discretely sampled, and the sampled values are quantized to a discrete set of integer values. The CCD camera measures the intensity of light transmitted through the gel and records the logarithm of each value. The image is stored as a file consisting of rows of numbers [pixels (picture elements)]. Each row of numbers consists of a string of numbers. For an 8-bit system, the numbers range in value from 0 to 255. The values for each number in the matrix represent the gray scale values of the digitized image.

Of all the available data acquisition devices, the CCD-based camera is the most versatile. It can be utilized for a variety of stained gels (Coomassie Brilliant Blue, silver, colloidal gold, ethidium bromide), autoradiographs, electroblots, and can even dynamically acquire images of gels developing in trays. Laser scanners are insensitive to red and are thus poorly equipped to handle colloidal gold-stained electroblots, as well as some silver stains.

2.2. Document scanners and video camera-based systems

Document scanners consist of a 1D array of detectors [38]. The array can be thought of as a "narrow CCD chip" that is physically moved across the gel. As the gel is scanned, light is bounced off the image and reflected back to the CCD chip, which records the light intensity as described for the CCD camera. The computer assembles this continuous scan into a 2D array of numbers. Generally, document scanners have more detectors along their length than the width of the standard 2D array in the CCD chip. Changing magnification can be performed within

the software package and simply involves changing the mechanical scanner speed. With the 2D CCD camera, changing magnification involves physically changing the lens of the camera or adding extension tubes.

Thermionic-tube based systems (Vidicon tubes) are functionally similar to CCD-based systems and have largely been replaced by the newer technology [37]. Electrons from a heated element travel through a vacuum to a sensitive faceplate, but are deflected on the way to form a raster pattern. The electron beam is scanned over the photosensitive surface of the face plate in two dimensions. The electrical output of the tube varies with the amount of light falling on the light-sensitive layer of the faceplate being scanned. The light-sensitive layer on the faceplate is typically composed of antimony sulfide, lead oxide or zinc and cadmium tellurides [39]. The sensitivity to amount and wavelength range of light is dictated by the composition of the layer on the faceplate.

CCD cameras, document scanners and Vidicon cameras are more susceptible to gray scale saturation effects than laser scanners [40]. They are generally 8-bit digitizers with maximum usable absorbance (A) range of 1.8–2.0 AU. Some cooled CCD cameras with 12- or 16-bit digitizers provide a wider linear range but are still logarithmic at the high end of the A scale [40]. Laser scanners with photomultiplier detectors can be linear over their entire A range.

2.3. Phosphor imagers

Commercially available phosphor storage imaging plates are composed of fine phosphor crystals of $BaFBr:Eu^{2+}$ in an organic binder [41,42]. High energy radiation from the sample excites electrons of the Eu^{2+} ion into the conduction band of the phosphor crystals. The electrons are then trapped in temporary color centers (F centers) of the $BaFBr^{-}$ complex with a resultant oxidation of Eu^{2+} to Eu^{3+}. The Eu^{3+} constitutes the latent image of the radioactive sample. The excited $BaFBr^{-}$ complex exhibits a distinct absorption band centered at approximately 600 nm. Exposing the excited complex to red light from a helium–neon laser (633 nm) releases the electrons from the bromine vacancies in the lattice back to the conduction band of the crystal, reducing Eu^{3+} to Eu^{2+*}. Eu^{2+*} then releases a photon at 390 nm as it returns to ground state. The intensity of the europium luminescence at 390 nm is measured and stored digitally in relation to the position of a scanning laser beam, resulting in a quantitative representation of the latent image formed on the storage phosphor plate by the original radioactivity from the sample. The residual image on the phosphor plate can be erased by irradiation with visible light and the plate is then ready for a new exposure.

The principal disadvantages of storage phosphor imaging are the significant instrumentation cost, susceptibility to signal fade, very large image data files and incompatibility with certain radioisotopes. The storage phosphor loses signal strength as a function of time ("signal fade"). Approximately 20% of the signal on the imaging plate can be lost after only 3 h [41,43]. Even the time taken to scan a plate can have a significant impact on the accuracy of the data, if a short exposure time is used [44]. Though fade can be a problem for short exposures, it is not an issue for standard 2D gel exposures of 17–72 h [43]. Loss of signal is reported to be between 30 and 46% after 3 days to 2 months delay in plate reading [41,42]. Among the commonly used isotopes, only tritium is too weak to penetrate the thin protective coating used on storage phosphor plates [41]. Standard image sizes generated by commercial phosphor imagers range from 10–40 Mb and are thus not transferable to a floppy disk [41,45]. They are also difficult to work with utilizing current image presentation software packages.

The principal advantages of storage phosphor imaging are increased sensitivity, good spatial resolution of signal and greater linear dynamic range of response. The response range of the storage phosphor system is approximately 10^5 to 1 compared to $3 \cdot 10^2$ to 1 for conventional X-ray film [41]. Storage phosphor imaging of ^{35}S- or ^{14}C-labeled samples is approximately 20–30 times as sensitive as conventional fluorographic

exposure [41,43]. For ^{32}P, storage phosphor imaging is 10 to 15 times as sensitive as conventional, low-temperature autoradiographic film exposure using intensifying screens [41,45].

Storage phosphor screens also have significant benefits when compared to conventional autoradiography for band detection combined with liquid scintillation spectroscopy for quantitation of radioactivity [45]. Background is much lower, providing increased ability to detect very small amounts of radioactivity. The storage phosphor screen allows more accurate mapping of radioactive spots than afforded by cutting bands out based upon alignment of an autoradiographic film. It provides a permanent high-resolution electronic record of the distribution and intensity of the radioactivity [45]. Spatial resolution has been estimated to be 290 μm for ^{14}C and 380 μm for ^{32}P [41]. Though liquid scintillation spectroscopy is superior with respect to differentiating between the energies of different radioisotopes in dual-labeling experiments, storage phosphor technology has been shown to have the ability to reveal ^{32}P signal from $^{35}S/^{32}P$ double-labeled sample by appropriate shielding with copper foil during some exposures [46,47].

2.4. Microchannel plate analyzers

A method to directly digitize miniaturized 2D gels (shrunken in 95% ethanol) was reported several years ago, that utilized a microchannel plate analyzer [48]. The original system required gels to be dried, coated with gold and placed in a vacuum chamber. Advancements in the development of microchannel devices, including the addition of inert gas to the detectors have made the technology of more use for routine quantitation of β-rays. Elaborate preparation of the gel is no longer required, it is placed directly under the detector array. Microchannel array detection has been successfully applied to the quantitation of 1D and 2D thin-layer chromatograms, in chloramphenicol acetyl transferase assays, Northern blot hybridizations, and the analysis of radiolabeled tissue sections [49,50].

The microchannel array detector, as an alternative to storage phosphor technology, provides direct electronic detection and real-time imaging of radioactively labeled material [49,51]. The microchannel array plate is a laminated structure with alternating conductive and non-conductive layers. A voltage step gradient is imposed on the successive conductive layers to produce an electric field of approximately 600 V/mm. β-Particles, emitted from the sample, pass through protective windows of the microchannels and ionize argon gas containing trace amounts of CO_2 and isobutane. The resulting electrons are accelerated by the high electric field in the microchannel, causing further ionization of the gas. The electron cloud migrates up the electric field gradient into a multiwire chamber. The multiwire chamber consists of a plane of anode wires and two perpendicular planes of metallic cathode tracks, corresponding to x and y coordinates. A further cascade amplification occurs in the high electric field around the anode wires, resulting in electric pulses in the x- and y-cathode tracks. The resulting signals in the cathode tracks are digitized and transferred to a digital signal processor.

As with liquid scintillation spectroscopy, data are reported as counts per minute (cpm) with statistical precision measurements. Cpm values are independent of counting time. Thus, data collected from long and short exposures can be directly compared, without the need for conversions utilizing internal standards. Images can often be acquired in only minutes, images can be monitored as they form, and acquisition can be terminated once sufficient information has been collected. Since β-rays are collected in real-time, the microchannel array system is not susceptible to image fade. The microchannel array detector exhibits excellent sensitivity and linearity. The linear response range of the system is approximately 10^5 to 1 with 3 dpm/mm^2 of ^{14}C detectable in 30 min and 0.3 dpm/mm^2 detectable in 16 h. Approximately 0.2 dpm/mm^2 of ^{32}P are detectable in under 10 min. The Packard Instruments InstantImager (Meriden, CT, USA) collects cpm data with a 16-bit capacity. The system automatically checks for saturation and saves a copy of the profile before any channel's capacity is exceeded. The principal problem with mi-

crochannel array detectors is the lower spatial resolution compared with standard autoradiography [37]. The Packard system has a 20×24 cm^2 microchannel array detector with approximately 200 000 discrete detection elements. This corresponds to a 400×400 pixel resolution for a 20×20 cm gel, which is a bit coarse for standard 2D gel electrophoretic imaging. Smaller gels will utilize a smaller portion of the detector and thus have correspondingly lower resolution. Fig. 2 shows a 2D gel imaged with a microchannel array detector. A final aspect to consider when comparing electronic imaging of radioactivity with using conventional film is throughput. If a modest sized experiment is performed with ten gels, the investigator can place all ten gels next to film for 17 h and then expose them. Alternatively, with the electronic method, a gel must be placed next to the detector, imaged for 1–3 h and the next gel placed next to the detector. Collecting data on all 10 gels requires 10–30 h effort.

2.5. Visualizing unstained gels

Proteins in unstained gels have been visualized utilizing ultraviolet (UV) imaging densitometry as well as by electric birefringence imaging [52,53]. UV imaging densitometry is based upon the absorption of UV light by proteins at 280 nm, which is primarily a function of the tyrosine and tryptophan content of the protein, or at 230 nm which is due to the peptide bond itself [13]. While the method is simple, relatively large amounts of protein are needed for quantitation. Sensitivity is also compromised because the polyacrylamide matrix and carrier ampholytes absorb in the UV region. The detection of cytochrome *c* by UV imaging densitometry is about 1/40th as sensitive as by Coomassie Brilliant Blue dye staining [52]. Though the UV absorbance of cytochrome *c* increases 10-fold when measurements are made at 230 nm instead of 280 nm, this is nullified by the fact that polyacrylamide absorbance at 230 nm is 40 times that obtained at 280 nm. Electric birefringence imaging measures induced linear birefringence generated by oriented charged, anisotropic molecules in an electric field (see [53] and references cited therein). Buffer boundaries and hydrodynamic fluid flow are also visible utilizing the technique, making it a valuable diagnostic tool for the study of the electrophoretic process itself. The visualization technique is roughly as sensitive as Coomassie Brilliant Blue staining but is often difficult to interpret due to the myriad of buffer fronts visualized along with the protein bands.

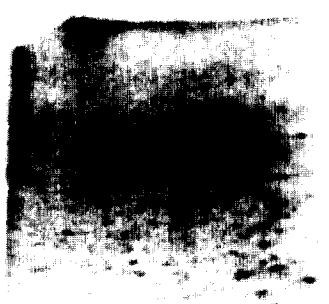

Fig. 2. Detection of [^{35}S]methionine radiolabeled proteins using a multichannel array detector (Packard Instruments). A miniaturized 2D gel (8.75 cm × 7.5 cm) was used in the study. Approximately 150 proteins were resolved in this 3-h exposure. Resolution would be expected to increase by 6-fold if large format, 20 cm × 20 cm, gels were utilized in the separation. Figure courtesy of Dr. Phillip Cash, Department of Bacteriology at Forrester Hill Hospital, Aberdeen, UK.

3. Semi-automated gel analysis systems

3.1. Image acquisition versus image analysis

A point that escapes many newcomers to image analysis is that the input device is not the analysis device. The CCD camera, document scanner, laser scanner, multichannel array device and phosphor imager are simply taking a picture of the gel. Analysis is performed with the image analysis software. Many sophisticated image acquisition devices are supplied with extremely rudimentary analysis software that require the user to physically outline each spot for quantitation. The creation of gel databases is out of the question with such systems. A number of semi-automated systems for the analysis and databas-

ing of 2D gels have been introduced in recent years including TYCHO, QUEST, GELLAB, HERMeS, GESA, Bio Image, MELANIE and ELSIE (reviewed in [26] and [54]). Cross-platform comparisons of the different systems is difficult and no one individual has expert capabilities in utilizing all the systems available. The acquisition device should be a secondary consideration as most analysis systems can be coaxed to work with almost any input device.

3.2. Database system requirements

In order to establish a high-resolution protein database one minimally requires an accurate determination of pI, M_r and quantity of protein present. Alternatively, a polar coordinate system specifying a direction vector and a scalar distance for each spot relative to some spot in the profile has been utilized by a few laboratories [26,55]. Given that 2D gel electrophoresis is based upon orthogonal separations, it would seem more reasonable to utilize a Cartesian coordinate system than a polar coordinate system to describe spot position. The polar coordinate system is dependent upon the lengths of the first and second dimensions which are not standardized among laboratories performing 2D gel electrophoresis.

Every year, there seems to be a further propagation in the number of computer-assisted gel analysis systems. Members from one laboratory leave and then develop their own flavor of the software along separate paths from the "mother" laboratory, a process akin to divergent evolution. Many of these systems also have counterparts under development in the commercial sector, adding to the multiplicity of programs. Weaknesses in a particular platform, when detected, are usually rectified in the next version of the software.

Bio Image (Bio Image Products, Ann Arbor, MI, USA), the system I have utilized most extensively, was primarily developed in the commercial arena and can thus be considered a closed system. This does not provide the investigator with the flexibility to add preprocessors and postprocessors to the software since the source code, file formats and data input/output conventions are not available. On the other hand, the user interface is generally better in commercial programs, customer support is available, and good ideas for improving the software are usually welcomed and implemented by the company's software engineers, which allows the investigator to concentrate on biology instead of computer programming. While not existing in as many incarnations as some of the other programs, several variant forms do inevitably arise from customers failing to maintain licensing agreements and thus running older versions of the program. Fig. 3 provides a very simplified view of the steps required to construct a 2D database. It is based upon the Bio Image software but many other systems utilize similar steps. It is presented to aid the reader in understanding the subsequent discussion on image processing.

4. Segmentation (digitization, image processing)

4.1. Resolution

Gels can be scanned at various levels of resolution. If the resolution is too low, significant information is lost, if too high, an excessive amount of data will have to be stored and manipulated for each image [26]. I routinely utilize 1024×1024 pixel image resolution, since gels can conveniently fit on a floppy disk. This is especially valuable for investigators that do not have access to cross-platform Ethernet networks, and would like to manually transfer an image from the dedicated imaging system to a microcomputer (often referred to as using the "Sneaker-net"). With an appropriate zoom lens attached to a CCD-based camera, images of even the smallest format gels (minigels) can be obtained at 1024×1024 pixel resolution.

4.2. Noise and artifacts

4.2.1. Effect of noise on spot detection; image corrupting (noise-making) filter

In general, a second-derivative or Laplacian analysis is utilized in detecting spot cores, the first step in finding spots. The Laplacian tends to

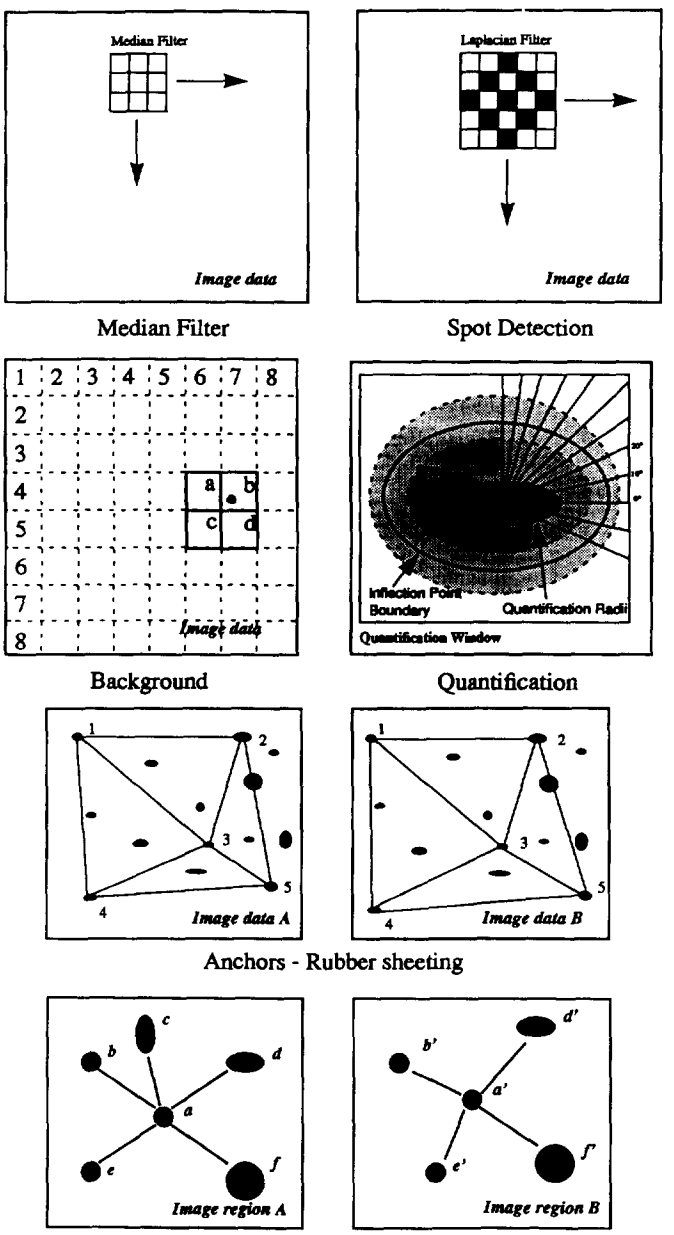

Fig. 3. Construction of 2D gel databases utilizing a representative image analysis system (Bio Image). Median filtering is performed to reduce spurious noise from the gel image. A Laplacian filtering method is used to locate spot centers. Background is calculated based upon an analysis of subregions of the gel. Spot quantitation is achieved by detecting inflection points for each of 36 radii propagated from the spot center. The spot boundary is determined by connecting the inflection points for each radius. Then the intensity values of all pixels within a spot boundary are summed and normalized by the pixel resolution to form the quantification value. Landmarks (anchors) are used to define common spots across sets of gel images. A triangle network is constructed and the images are transformed to a common coordinate system (an overlay plot). Finally, constellation matching uses the triangle network to find similar regions in a set of images. The distortion of each constellation on the study image is compared with the original constellation on the reference gel. Spots requiring the lowest distortion, above a set threshold, are defined as matched.

amplify image noise, and it is thus necessary to remove high-frequency noise before computing the Laplacian. This is generally performed by convolution or median filtering [56–58]. The effect of noise on spot detection is shown in Fig. 4. Very modest levels of noise introduced into an image significantly reduces the number of spots detectable by the Laplacian filter.

Noise generated by the scanning process itself can be reduced by physically acquiring the image several times and averaging the results. A microcomputer-based system I previously employed for 2D gel analysis scanned a gel 32 times to obtain a confidence level of one gray scale level of the total 256 levels available [59,60]. Most computerized gel imaging systems acquire information for each pixel only once so that some noise is associated with each pixel value. An evaluation of an image of a gray scale wedge revealed that the Bio Image system assigned gray scale values with an accuracy of ± 4 gray scale levels (± 1.56%) of the total 256 levels available. While this level of noise is very low, it is sufficient to interfere with detection of the lowest abundance polypeptides by the Laplacian spot finder and system performance can be significantly improved by application of certain convolution or median filtering techniques.

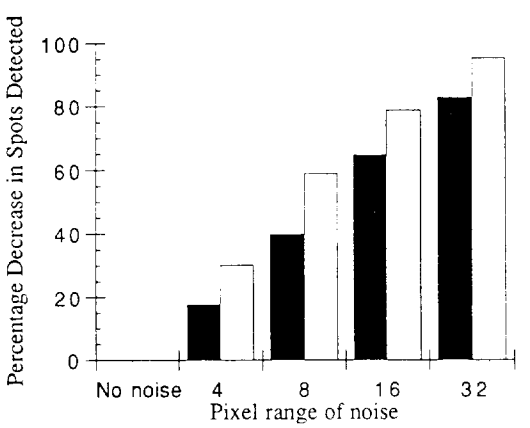

Fig. 4. Influence of noise on the performance of the Laplacian spot finding algorithm. Various levels of uniformly (■) or Gaussian (□) distributed noise were added to a standard 2D gel image utilizing filters available from Adobe Photoshop (Adobe Systems, Mountain View, CA, USA). The Bio Image Laplacian spot finding algorithm was then applied to the noisy images. The total number of spots found in each noisy image was then compared with the number of spots found in the unaltered image.

4.2.2. Improving performance with area processing filters

Convolution filtering can be thought of as a weighted summation process [61]. The group of pixels utilized in the filtering process are referred to as the neighborhood. The neighborhood is generally a 2D matrix of pixel values with each dimension having an odd number of elements [61]. During convolution filtering, the gray scale value of a pixel is transformed by a rule which takes into account the values of these neighboring pixels. For example, in a 3×3 matrix of pixels, the center pixel is replaced by reference to the gray scale levels of its eight neighbors as well as its own original value. Median filtering is another area processing technique distinct from convolution filtering. Instead of utilizing an algorithm to assign the value of the central pixel, the pixels in the neighborhood of the pixel of interest are sorted and the median pixel value is then assigned to the central pixel. In the past, the Bio Image software has allowed implementation of a 5-point median filter as an option applied during the image acquisition process. This is similar to the standard 3×3 median filter except that only the four nearest neighbors diagonal to the pixel of interest are utilized in determining the new pixel value. The 5-point filter was found to generate artifactual patterning of low intensity pixels, which interfered with accurate quantitation of low abundance polypeptides and is thus no longer recommended as a noise-removing filter for gel analysis [58].

In general, larger sampling convolution matrices tend to remove local, high-frequency noise in adjacent pixels more effectively than smaller ones. When the filter is too large, however, significant data may be lost. We have found that two of the most successful convolution filters for noise removal from 1024×1024 pixel images of large format gels are a previously described 7×7 pixel least squares best fit template and a 7×7 pixel Gaussian template [54,62]. The filters are shown in Fig. 5. The most significant effect

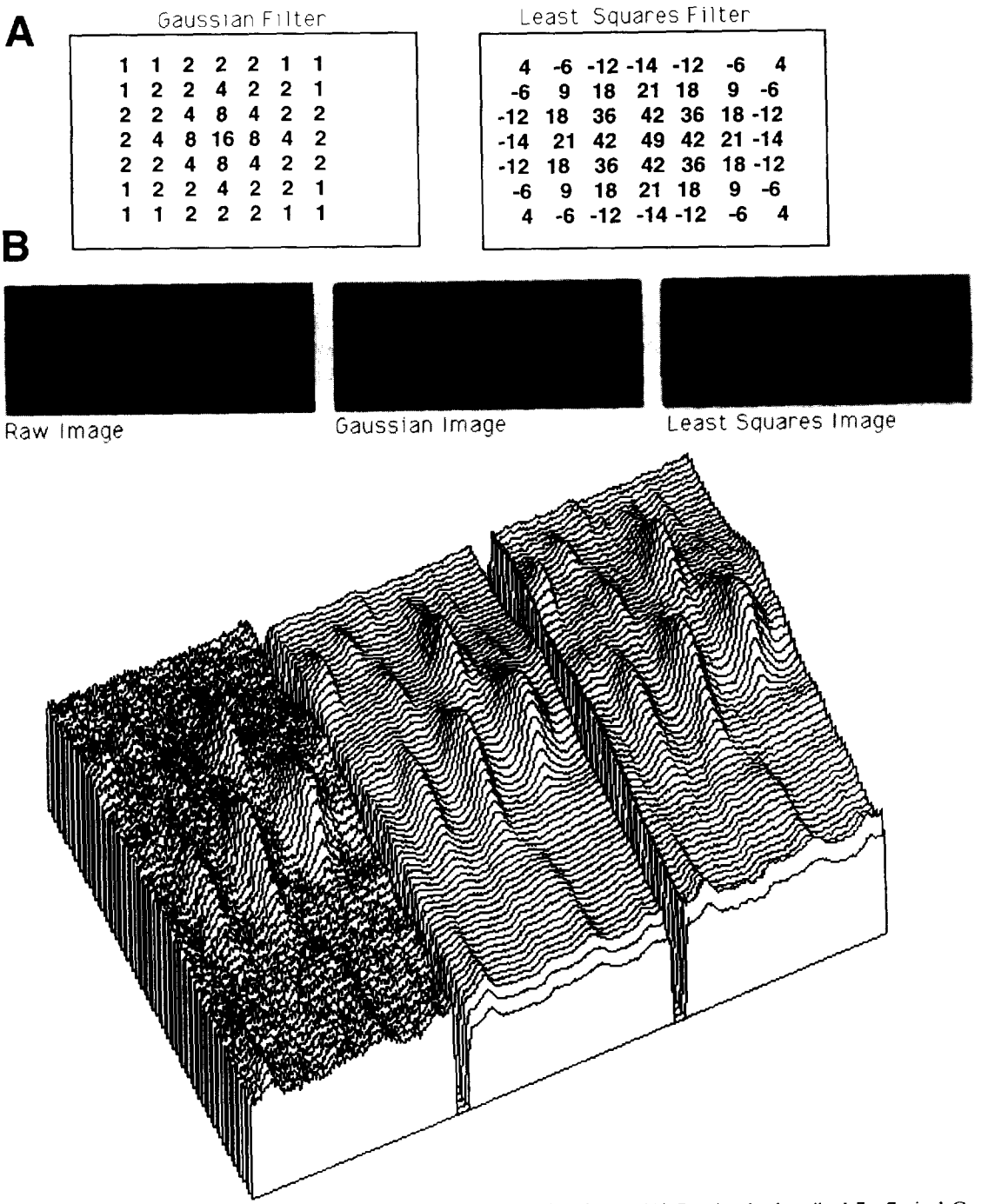

Fig. 5. Reduction of noise in a gel image by application of convolution filters. (A) Previously described 7×7 pixel Gaussian template (left) and 7×7 least squares best fit template (right) used for noise elimination [54,62]. (B) The left-hand image and three-dimensional projection show a portion of a 2D gel digitized at 1024×1024 pixel resolution using a CCD-based camera. The middle image and three-dimensional projection show the results of applying the Gaussian template to the image. The right-hand image and three-dimensional projection show the results of applying the least squares best fit template to the image. Note that while visual inspection fails to reveal significant differences between the gels, the noise associated with the original image, appearing as jagged lines in the three-dimensional projection, has been removed in the processed images.

observed after convolution or median filtering is that many more low abundance polypeptides are resolved from background noise. We observed a 60–65% increase in polypeptides in a typical silver-stained gel after applying these techniques [58].

The choice of filters depends somewhat upon the type of gel image being analyzed. Sequential digestion of genomic DNA with two different restriction enzymes has been used to generate 2D agarose patterns [63,64]. Multiple fragments are visualized as spots by Southern analysis with probes containing repetitive genomic sequences. The patterns obtained from the procedure are characterized by diffuse, weak signal spots and highly textured image noise. An image-processing filter specifically designed for analysis of such spots was recently reported [65]. Averaged 3×3 "super pixel" values are utilized instead of single pixels for each element of the Laplacian convolution filter to make the process more immune to high spatial frequency noise. It is unclear whether or not the same results could be achieved utilizing standard convolution filters on images acquired at lower resolution.

4.2.3. Erosion-dilation methods

Erosion-dilation methods are generally utilized in conjunction with systems that rely upon a spot model (parametric analysis) [54,55]. As an example, a Gaussian spot model is assumed for the proteins and any boundary pixels that do not fit the model are removed (spot erosion). Then a series of dilation steps are performed to expand the remaining pixels that represent the spots. Noise is removed by ignoring any data that does not fit the spot model. Streaks can also be modeled, and once identified, removed from the image.

5. Spot/band detection (background, boundaries)

5.1. Background determination

Many minicomputer-based image analysis systems determine gel background by normalizing the low intensity pixels in various subregions of a gel and then automatically subtracting this normalized value from all of the pixel data generated for the gel [56,66]. In an alternative procedure, a frequency histogram is generated for different regions of the gel [67]. Then a Gaussian curve is fitted to the low-intensity end of each histogram. The frequency maximum of the Gaussian curve is used as the background value for the specific region it was generated from. For regions that are densely populated by spots this method of background estimation does not perform well. The system detects these problem regions and substitutes the Gaussian estimate with an interpolated Gaussian estimate derived from surrounding regions. The Bio Image system calculates background based upon pixels with "flat" Laplacian values (regions where the second derivative of gray scale is zero). Dark artifacts are eliminated from this determination by scoring the background as the most frequently found value (mode) rather than the mean value. Some systems simply utilize background thresholding in their spot analyses [25,59]. QUEST defines background for each line of data and subtracts it before finding the spots, while the Mariash system requires the user to determine the background intensity threshold manually for each region scanned by adjusting potentiometers on the digitizing circuit board.

5.2. Manual versus automated detection

Automatic spot detection and quantitation by computer is critical for comparisons of proteins across many gels. The computer reproducibly executes procedures for determining spot boundaries, an important requirement for integration of the spot volume and thus determination of protein amount. Manual assignments of spot boundaries, on the other hand, are very difficult to perform identically from gel to gel. This is clearly evident from a study of multiple determinations of the IA of a single, well resolved spot and a spot belonging to a cluster of four poorly resolved spots (actin isoforms) from a single gel performed manually and using the Bio Image software (Fig. 6). Three individuals

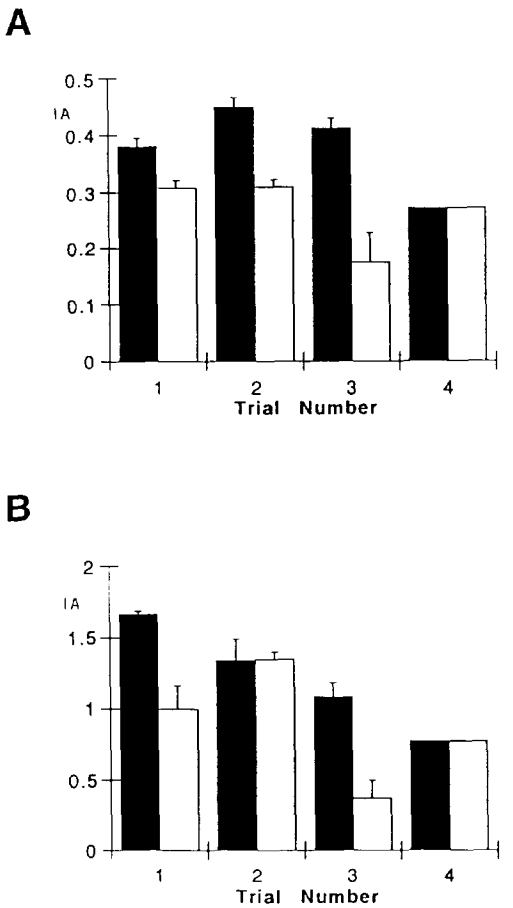

Fig. 6. Variability in manual spot boundary determination by individuals with different levels of experience in gel electrophoresis and image analysis. Two spots were evaluated: (A) a well separated, round spot and (B) an actin isoform that was a component of a cluster of spots. Trial 1 was performed by an individual with a high level of expertise in both electrophoresis and imaging, trial 2 by an individual with experience in electrophoresis but not image analysis, trial 3 by an individual without prior experience in either electrophoresis or image analysis and trial 4 by the Bio Image Laplacian spot finder. Each participant determined the spot boundary for each spot 3–5 times. Images were displayed as gray scale (■) and pseudocolor (□) representations to further evaluate variability in spot boundary assignment. The mean integrated absorbance (IA) is shown for each group, as well as the standard deviation in the determinations.

were selected to perform the experiment; (1) an individual with extensive experience in performing electrophoretic separations and computer-assisted analysis of gels, (2) an individual with extensive experience in running gels but little background in their analysis by computer, and (3) an individual with extensive background in oligonucleotide and peptide synthesis but no experience at all in electrophoresis or image analysis. As can be seen in Fig. 6, manual assignment of spot boundaries introduced significant irreproducibility into the spot quantitation process. Furthermore, the choice of display format (gray scale versus pseudocolor) had a significant impact on manual selection of spot boundary. Different individuals selected spot boundaries by different criteria, prohibiting the construction of gel databases with a team of workers. The computer created the spot boundaries in an identical manner for each determination and thus there was no variation in the computer measurements at all.

5.2.1. Spot segmentation tests

Three major groups of tests have been developed to evaluate the reliability, reproducibility and precision of computerized gel analysis systems [68]. The scanner tests evaluate the stability and reproducibility of the input device by evaluating scanner output as a function of time, and consistency of the output at different points in the scanning field. Computer-generated ideal spots are used to determine the system's ability to separate closely spaced and partially merged (shoulder) spots, the ability to deal with random noise and the ability to handle streaking and other commonly encountered phenomena. The real gel images are used to evaluate noise introduced by scanning, accuracy of background detection, and the reproducibility of the actual quantitative measurement of protein amount between gels.

5.3. Determination of spot boundaries (parametric versus non-parametric methods)

The computer-assisted gel analysis systems were, in general, developed independently and often use completely different approaches with respect to spot detection. The critical task in quantitative 2D gel analysis is determining spot boundaries. The computerized gel analysis systems can be classified into two broad categories

with respect to this task; parametric and non-parametric methods. The QUEST, TYCHO and HERMeS systems utilize parametric methods while the ELSIE, GESA, MELANIE, Bio Image and GELLAB systems utilize non-parametric methods (reviewed in [54]). Parametric systems model spots as 2D Gaussian distributions, while non-parametric systems assume no explicit model of spot shape except that there is a peak surrounded by decreasing density. Actual spots often deviate significantly from the idealized Gaussian model. This deviation has been attributed to the fact that polypeptides have a tendency to repel and distort each other during electrophoresis [68]. The local electric fields formed by the ampholine-like polypeptides perturb the local fields of adjacent polypeptides.

The decomposition and mathematical modeling of complex patterns is not a trivial task [69]. Recently, seven functions were compared for their ability to model 1D gel electrophoretic band peaks [69]. Bands were best modeled by asymmetrical functions such as asymmetrical Gaussian or Gaussian–Cauchy functions though several of the other functions provided better approximations for specific bands in the electropherogram. To my knowledge, similar experiments have not been performed for 2D protein patterns, though QUEST utilizes a symmetrical and HERMeS utilizes an asymmetrical Gaussian model for spot shape [25,55].

5.3.1. First- and second-derivative analyses

Two general approaches have been taken with respect to non-parametric spot detection; first- and second-derivative gray scale analysis (Fig. 7). A microcomputer-based system I used extensively in the past detects spots utilizing the first derivative of the gray scale values [59]. The system scans an image up to 256 times, digitizes the signal, and stores the information as an intensity matrix in the microcomputer's memory. The intensity matrix is then converted in to a minimum map which defines spot boundaries. An individual spot contour is defined as an area bounded by minimum intensities in at least two orthogonal axes. The intensity matrix is examined for threshold zeroes, relative minima,

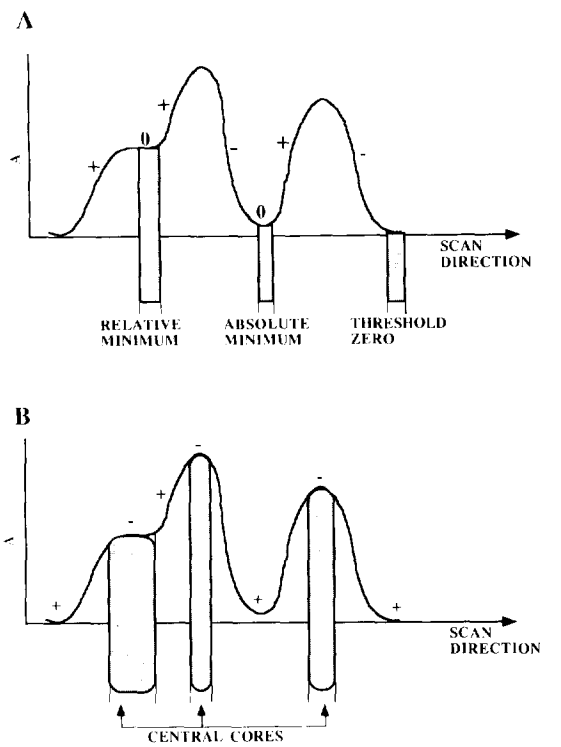

Fig. 7. Schematic representation of first- and second-derivative determinations of spots in a 2D image. The first-derivative determination is utilized to identify spot edges while the second derivative locates peak heights. (A) The first-derivative determination. The cited algorithm identifies relative minima, absolute minima and threshold zero values when finding spots [59]. A relative minimum is located by the pixel pair with zero slope whose adjoining pixel pairs produce slopes of identical but non-zero signs in the direction of scanning. (B) The second-derivative determination. Central cores corresponding to the negative second derivatives of gray scale density are located. Then ancillary algorithms check for monotonically decreasing gray scale values around the core in order to find the spot boundaries.

and absolute minima. These three types of minima are illustrated in Fig. 7A.

Most computer-assisted gel analysis systems utilize some type of second-derivative procedure for spot detection. A second-derivative (Laplacian) analysis of the gray scale surface differs from a first-derivative analysis in that spot centers are being detected instead of spot periphery. The Bio Image software utilizes a Laplacian spot finder to evaluate each pixel for changes in A propagating to its neighboring pixels in four

directions (x, y, and two 45° angles). In this central core detection procedure, the spot center is defined as those pixels having negative second derivatives of gray scale density. This is because the rate of increase of density as a spot is scanned from its edge to its center is less in the central core than at the preceding inflection point. This is illustrated in Fig. 7B. Ancillary algorithms add adjacent pixels to the central core subsequently. These algorithms search for monotonically decreasing values of gray scale intensity until the background of the gel is reached. Finally, spot boundaries are demarcated after evaluating 36 radii generated from the spot center. The zero cross of the second derivative of the gray scale values (z-axis curvature) is determined and then the 36 points established are connected to generate the actual spot boundary.

5.3.2. Head-to-head comparison

Few direct comparisons among the different computerized gel imaging platforms have been undertaken. The systems are inherently quite expensive and it is rare for an institution to have even a single system, let alone a collection of them. There is a real need in the field for an impartial evaluation of the leading systems, much as is done for hard drives, optical character recognition software, and laser printers in various computer trade magazines. Perhaps, this task could best be accomplished by organizations such as the International Electrophoresis Society and its affiliates.

Recently, two high-end, non-parametric imaging systems, Bio Image Visage 2000 and GELLAB-II were evaluated [70]. These systems are both quite sophisticated, and are among the best systems currently available. A set of 29 silver-stained gels from a study of urinary proteins in metal recovery plant workers with confirmed body burdens of cadmium were utilized in the analysis of the two imaging systems. It should be noted that urinary protein gel profiles are unusual in that they are characterized by several charge trains of very abundant components and some very minor components. A typical cell lysate, from endothelial cells for example, would have many minor proteins and only a couple high abundance proteins (actin, vimentin). To eliminate any camera or scanning differences, the same set of image files were analyzed with each system, after first converting the files to each system's required data storage format. The study compared the capability of the two systems to detect, quantify, and perform gel-to-gel matching of silver-stained protein spots. The ability of each system to detect candidate protein biomarkers for cadmium toxicity and the estimated labor intensiveness of deriving data from each system was also evaluated.

The Bio Image system detected 890 ± 178 spots while the GELLAB-II detected 1971 ± 199 spots. A great deal of the difference observed between the systems can probably be attributed to the fact that a 3×3 lowpass average filter was used by the GELLAB-II system for noise reduction while no filter was used in the Bio Image system. We have found that noise reduction filtering permits 60–65% more polypeptides to be detected in silver-stained gels by the Bio Image system [58]. It is readily apparent that the Bio Image system had more difficulty than the GELLAB-II system with proper quantitation of the larger spots (spots with areas of 3.0 ± 5.4 $mm^{2)}$ compared with the smaller ones (those with areas of 1.3 ± 0.7 mm^2).

5.3.3. Advances in spot boundary determination

A fast, non-parametric spot segmentation algorithm was recently reported that is both memory efficient and able to process large gel images in a reasonable amount of computation time on low-cost (i.e. reliable) computers [71]. The procedure utilizes the second derivative of an image to encode spot regions in a single raster scanning pass through the entire gel. The entire spot segmentation process is reported to require about 28 s with 1000 spots detected [71]. As the performance of microcomputers increases, it is expected that more sophisticated gel analysis programs will become more readily available to a wider spectrum of biological scientists.

Many modern imaging systems have difficulty in the quantitation of gel images containing both very large and very small spots. If spot detection parameters are adjusted to optimize detection of

the large spots, the small ones are not detected. If, on the other hand, parameters are adjusted to detect the small spots, then the large ones are incorrectly fragmented. Several laboratories are devising heuristic enhancements to conventional spot segmentation algorithms in order to correctly split large, nearly saturated or fully saturated, merged spots [40,72]. The Laplacian of such large spots poorly represents the shape of the spot's central core. This poor representation results in the fragmentation of the spots. A good solution to this problem is to first merge the fragments together and then split out separate spots based upon the shape of the initial merged spot. After the initial Laplacian spot detection phase, and the merging of suspect spots, a boundary analysis algorithm finds robust opposing concavities (saddle points) on the fused spot boundary which indicate the position where the merged spots should be divided into smaller ones. While merging and splitting spots is computationally intense, the process is only used on large spots that approach saturation density and the duration of the quantification process is not substantially increased.

5.4. Spot shape as a quality criterion

A useful criterion for assessing both the quality of the electrophoretic separation and the quality of the spot finding algorithm is spot shape. The Bio Image spot shape algorithm is as follows:

$$\text{Spot shape} = \text{integrated area}/[XY(\pi/4)]$$

In this equation, X is the diameter of the spot in the IEF direction, while Y is the diameter of the spot in the M_r direction. Spot shape has a range of 0–2. A circular spot has a value of 1, as do many ellipses. A spot with tailing in either dimension (or both) has a value less than 1. A fused cluster of spots has a value greater than 1. Spot shape is also useful as a signature for verification of correct spot matching. Two spots on different gels corresponding to the same protein will have similar spot shapes. If they do not, either the quality of the electrophoretic separation or the accuracy of the matching is brought into question.

6. Measurement (gray levels, mass and charge standards, calibration)

6.1. Number of gray levels versus image size compromise

6.1.1. Curve fitting and look-up tables

Regardless of the method of digitization, it is necessary to calibrate the raw intensity in order to obtain quantitative data expressed in AU, cpm or micrograms of protein. In all cases this final transformation of the data is not achieved by simply multiplying the raw intensity data by a simple constant as the raw intensity is not linearly related to the physical parameters. When using a densitometer as the input device, non-linear response is due to the non-linear film response curve of the autoradiograph. When a Vidicon-based camera is used as the input device, the non-linear response of the phototube also contributes to the non-linear relationship [39]. The signal current produced by the Vidicon tube is equal to the light intensity taken to some power γ. The γ of a camera is due to the non-linear response of the target semiconductor material to light. Most Vidicon tubes have γ values ranging between 0.6 and 0.8. In practical terms, regardless of whether the response curve is due solely to non-linearity of the film or due to a combination of the non-linearity of the film and the non-linear response of the detector, the problem is dealt with by generating a calibration curve. If one desires to express the data in cpm, this is done by making a gel with serial dilutions of polyacrylamide containing known amounts of radiolabeled proteins [25]. The radioactivity is quantified using a scintillation counter and strips of the calibration gel are included with 2D gels prior to autoradiography. The 2D gel data are then scanned and the raw intensity is converted to physical units by means of a look up table (LUT) embedded in the gel analysis program or by means of a non-linear curve-fitting equation that describes the calibration curve such as

Rodbard et al.'s four-parameter logistic–log transformation, shown below [73,74].

$$Y = \frac{a - d}{1 + (X/c)^b} + d$$

The response curve is sigmoidal in shape and can be characterized by an upper plateau, a lower plateau, a slope factor and a midpoint. In the equation shown, X is the raw intensity data and Y is the corrected intensity expressed in AU, cpm, or micrograms. The response for zero dose is represented by a in the equation, the response at infinite (saturating) dose is represented by d, and the response half way between the zero and infinite dose response is represented by c. The slope at the half way point of the standard curve is represented by b in the equation. Generally, it is quicker to precalculate a table of function results and look them up for each pixel in the image than to compute the values directly each time a new pixel is encountered. Thus, most systems utilize LUTs.

6.1.2. How many gray levels is enough?

Gray scale information has commonly been collected using 6-, 8-, and 12-bit A/D converters, corresponding to 64, 256 and 4096 discrete shades of gray. Most of us can probably conveniently describe only 2 bits of gray scale information, i.e. black, dark gray, light gray and white. If one considers an A range of 0 to 4 units, then the uncertainty in a measurement for a 6-bit scanner is 4/64 or 0.0625. For an 8-bit scanner the uncertainty is 4/256 or 0.016 and for a 12-bit scanner it is 4/4096 or 0.001. For an A of 0.10, this translates into a percentage uncertainty of 62.5% for the 6-bit scanner, 16% for the 8-bit scanner and 1.0% for the 12-bit scanner. The uncertainty in gray scale measurement is depicted graphically in Fig. 8. Most state-of-the-art densitometers utilize 8- or 12-bit A/D converters. The performance of 8-bit and 12-bit scanners differ markedly only at the very lowest A levels, i.e. for barely visible spots consisting of pixels of 0.01 A. These spots are the least accessible to all modern bioanalytical techniques, as well. They are unlikely to be detectable by

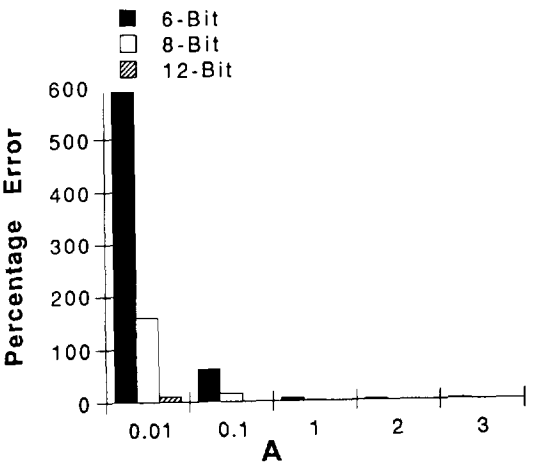

Fig. 8. Percentage uncertainty in the measurement of absorbance (A) values utilizing 6-, 8- and 12- bit data acquisition devices. While 6-bit data acquisition provides only semi-quantitative results, 8-bit data acquisition provides accurate measurements of gray scale values for all but the very-lowest-intensity spots, and 12-bit data acquisition provides exquisite sensitivity and accuracy for even very-low-intensity spots.

immunoblotting, cannot be subjected to protein microsequencing and are very difficult to purify with confidence, especially in the absence of any bioassay. Being able to point at a barely detectable spot and say "I am confident that this one increases by 50% in the treatment group" is of dubious value. Without substantial purification, research on that particular protein has reached a dead end. The 2D gel literature is littered with publications showing a gel, with an arrow pointing to a spot and captioned "this went up".

6.1.3. Image portability and usability

Recording data in terms of 8 bits per pixel rather than 12 bits greatly reduces the space needed to store scans and, in general, no significant difference in results has been demonstrated [68]. Additionally, the images are easily transferred to desktop publishing and image processing software. Recently, a commercial laser densitometer has been provided with the capability of scanning in both 8- and 12-bit file formats, allowing one the exquisite sensitivity for low-A spots as well as a convenient presentation format [75]. This solution does not alleviate the need for very high capacity data storage, however.

6.2. Molecular mass estimation, the physics and the biology of the situation

In SDS-PAGE, M_r estimation is generally based upon comparison of unknown proteins with lanes of protein standards or with proteins within the sample having known M_r. A plot of $\log_{10} M_r$ versus relative mobility (R_F) yields a straight-line relationship over a restricted M_r range, and the M_r values of the unknown proteins are determined by interpolation. The linear range of such graphs is approximately M_r 12 000–45 000 for 15% polyacrylamide gels, 15 000–70 000 for 10% polyacrylamide gels and 25 000–200 000 for 5% polyacrylamide gels [76]. The M_r values for the markers are often derived from gel filtration chromatography and related procedures. We have found these values to be too inaccurate for many of our studies. A comparison of M_r values for several proteins (actin, the tubulins, vimentin, vinculin, and PCNA/cyclin) indicated that the gene sequence-derived M_r estimates differed from the electrophoretic estimates by 3 to 17%. In terms of the polypeptides commonly studied by 2D gel electrophoresis, these discrepancies are very significant. For example, the M_r values of cytokeratin 7 and 8 differ by 4.2%, cytokeratin 19 and actin differ by 5.3%, and α-tubulin and β-tubulin differ by only 0.6%. With the widespread availability of computerized statistical packages, it has become less important that the M_r function be modeled by a straight line.

6.2.1. Polynomial functions versus logarithmic approximation

We and others generated polynomial equations for calculating M_r values over a broader spectrum of mass ranges [60,77]. These M_r functions require the user to specify at least two known M_r values (from the M_r standard lane or, better yet, based upon known mobilities of species in the 2D gel) and assigns M_r values to all other proteins in the scanning area. Most commercial systems have similar algorithms, the Bio Image system using multiple standards and determining the M_r values of the unknown spots using a $\log_{10}$ function. Winston fitted $\log_{10}$ versus R_F plots by polynomial regression analysis [78]. He reported that a third-order polynomial was capable of predicted M_r values from 14 400–97 400 with a maximum error of 1% using 12% polyacrylamide gels. The linear fit to the $\log_{10}$ plot of the data, on the other hand, generated a maximum error of 17% over the same M_r range. We performed regressional analysis of M_r versus R_F plots for three polyacrylamide gel concentrations (5, 10 and 15%) [60]. The accuracy of the assigned M_r values was verified by evaluating commercial standards containing six proteins ranging from 205 000 to 29 000. The M_r values assigned to the proteins differed by an average of 3% from the literature values. Polynomial regression equations have also been devised for calculating the M_r values of proteins separated on gradient polyacrylamide gels [77].

Polynomial equations are subject to unstable behavior outside the observed range of data, and may unrealistically oscillate between the data points, thus not accurately describing the physical phenomenon being modeled [73]. Cubic spline and four-parameter logistic models are also suitable for estimating M_r values [73].

6.2.2. Globular versus fibrillar proteins

Recently we used gene-sequence calculated M_r data from the literature, to rank the major cytoskeletal polypeptides of human mesothelial cells from highest M_r to lowest M_r [79]. This rank order of sequence-calculated M_r values was compared to the rank order obtained from the actual migration of the polypeptides in different gel systems. The rank order obtained using Tris–N[tris(hydroxymethyl)methyl]glycine (Tricine) and the Tris–borate gel systems agreed with gene-sequence data. With the almost universally used pH 8.3 Tris–glycine system, many polypeptides migrated anomalously. The differences in the rank order of the polypeptides examined were due to shifts in the positions of the intermediate filament proteins. Based on an analysis of the 500 most abundant polypeptides in the human mesothelial cell lysate, the migration of 20% of the polypeptides was influenced by the differences in the buffer systems. Based on our studies, it appears that polypeptides with a high

α-helical content and long helices tend to migrate anomalously in the standard Tris–glycine system while those with low α-helical content and short helices migrate independently of gel running conditions.

Ferguson plots can also be used to estimate M_r [6,80,81]. A series of gels are run using different polyacrylamide concentrations or, alternatively, a single transverse-gradient polyacrylamide gel is utilized [6]. The mobility of the protein of interest is found for each gel concentration and a plot of $\log_{10}$ of R_F versus polymer concentration [% T; T = (g acrylamide + g N,N′-methylenebisacrylamide)/100 ml solution] is generated. The ordinate intercept of a Ferguson plot (Y_0) is a measure of protein mobility in free solution, while the slope of such a plot (K_r), is related to molecular size. The method is suitable for very simple samples containing only a few components but is not practical for 2D gels containing thousands of proteins. Changes in the electrophoretic buffer system, from Tris–borate to Tris–glycine, substantially alter the K_r values of proteins, altering M_r estimates (see [6] and references cited therein).

While it is possible to more accurately model the M_r function in electrophoretic separations using polynomial equations, deviations in protein migration from ideal behavior probably renders these efforts ineffectual. Proteins are not truly separated according to their M_r in SDS-PAGE. Separation is based upon the mass, the distribution of charges on the protein and any residual secondary structure maintained in the presence of the anionic detergent. Thus, I now routinely utilize a simple standard $\log_{10}$ function for estimating the M_r values of electrophoretically separated proteins.

6.3. Isoelectric focusing: the often neglected dimension

Polypeptides may migrate anomalously in IEF gels, but the phenomenon has not been rigorously studied to date. The IEF dimension is poorly characterized in most 2D profiles. Carrier ampholyte-generated gradients are never, strictly speaking, linear. Instead, they are sigmoidal in shape with the pH profile more shallow at the pH extremes than in the center of the gradient. IEF is susceptible to a number of phenomena including gradient decay with time due to the differential migration rates of hydrogen and hydroxide ions (cathode drift) [82]. Additionally, the polypeptides tend to influence the shape of the gradient, since they themselves are carrier ampholytes. Unfortunately, many investigators appear to guess the p*I* values of their proteins based upon the pH range of the carrier ampholyte they added to the acrylamide solution prior to gel polymerization. If the stated range on the bottle is 3–10, they assign these values to the two extremes of their gels and try to interpolate all of their protein p*I* values from these two ends. The procedure is ludicrous, as standard IEF in carrier ampholytes is only capable of resolving polypeptides with p*I* values in the range of 4.5 to 7.5. It is thought that disulfide reducing agents are responsible for the pH 7.5 limit of carrier ampholyte-mediated IEF [82]. Unlike with SDS-PAGE, convenient internal protein standards for IEF are not in widespread use. Some laboratories have utilized carbamylated proteins as internal standards but they obscure portions of the gel [83]. Additionally, the number of species resolved in the charge train depends upon the size of the gel and the spots in the charge train are diffuse and poorly defined [84]. The p*I* values are often determined in IEF utilizing external calibration with gel slices from a representative gel run in parallel with the gel containing the sample. Alternatively, p*I* values are determined utilizing well characterized components in the sample itself (actin, tubulin, vimentin, calmodulin, tropomyosin) [79]. The approximate p*I* values of all other proteins are established based upon linear interpolation between the standards. Recently, the p*I* values of 41 known proteins common to most human cell types were determined utilizing narrow-range immobilized pH gradient gel electrophoresis [85]. This procedure represents the best calibration of the IEF dimension to date. A convenient method for the transfer of known proteins from one gel system to another by elution and co-migration should facilitate the

propagation of internal standards between different cell types run on different gel systems [85].

7. Comparing (matching, editing, databasing)

7.1. Matching gel pairs

Gels are commonly matched using fully connected non-directional graphs (generalized Gabriel graphs) [26]. The reference and experimental gel are first superimposed and aligned globally using at least three user specified spots (landmarks, anchors) that are considered to match with high probability. Global alignment is computed using the least squares method to estimate horizontal and vertical distortion in the experimental gel. The generalized Gabriel graph algorithm is then run on the globally aligned gels and local alignment is computed utilizing the user specified matched landmarks. Unmatched spots are aligned next, utilizing all the nearest matched neighbors. Variations on this method of spot alignment have been implemented in a variety of systems. Approximately 2% of the spots in a gel image must be user specified utilizing the Bio Image software for satisfactory matching. Other systems may require as many as 10–15% of the spots to be user specified.

ELSIE and MELANIE utilize an automatic matching program that pairs spots in two given gel images by comparing their respective positions and sizes by a cluster-matching technique [86]. Starting with the most intense spots in a gel, the program determines if spots are equivalent by trying to match the cluster of neighboring spots from each image. The program then performs the same operation on the secondary clusters and proceeds until the majority of spots are matched. The remaining unmatched spots are then mapped into the coordinate system of the other gel using the matched spots as landmarks. The program has some difficulty in automatically selecting landmark spots when gel patterns are very complex. MELANIE uses a prematch feature that automatically finds landmarks in a subset of spots (i.e. moderate intensity spots only) prior to running the automatch routine [14]. MELANIE also allows for user defined landmarks, and matching by triangulation methods [14].

A unique approach to matching 2D gels was recently proposed that is based upon mapping every pixel of a reference gel image to the study gel image rather than simply matching the identified spots on each gel [87]. Disparity vectors are established for each pixel and the study gel image is then transformed by "warping" or "rubbersheeting" methods so that it will match the appropriate pixel in the reference gel. Spots are then identified by a series of morphological operations and conventional filtering techniques. An obvious drawback to the procedure is that it is computationally demanding. Instead of matching a thousand polypeptides, it is necessary to match 1–4 million pixels (depending on detector resolution) for each gel. The system is able to successfully match the spots between gels without intervention from a human observer but requires several hours to complete the match of a gel pair. For comparison, the Bio Image system can match two gels in 1–2 min. This approach and other "rubbersheeting" methods may become increasingly more feasible with advancements in computer processing speed.

7.1.1. Pincushion and barrel test

Identical 2D gel separations are not possible, even under the most rigorously controlled laboratory conditions. Thus, pairs of gels can never be precisely superimposed. During the matching process, corrections must be made for gel offset, axis rotation and local gel distortion. Most systems can easily match gels that differ only in their positioning on the scanning device. Gel distortion is a much more difficult problem for matching programs to deal with effectively. Pattern distortion in PAGE is a well recognized but rarely studied phenomenon. Until recently, no definitive studies on the matter had been published. A recent study examined a number of parameters including gel tank configuration, gel cooling, gel buffer composition, gel storage duration, electrical field strength, and temperature with respect to lane distortion in SDS- PAGE [88]. Outward lane distortions due to buffer

composition and electric field strength, as well as inward lane distortions due to collapse of the gel matrix were noted. These types of distortions present significant problems for 2D pattern matching algorithms. Lane distortion also significantly decreases the length of sequence information obtained using automated fluorescence-based DNA sequencers [89]. A number of algorithms for correction of the most common distortions in 1D gels, "smiling" and "frowning" artifacts, have been developed (see [90] and references cited therein).

While tests for the evaluation of the reliability, reproducibility and precision of computerized gel analysis systems have been developed, tests for the gel matching algorithms are lacking [68]. An appropriate set of images for the evaluation of matching algorithms is relatively easy to create once the distortion phenomenon is understood from a wet chemistry perspective (Fig. 9). Distortions in the first dimension primarily arise from stretching or compressing a portion of the IEF gel, as well as cathodic drift of the gradient. Distortions in the second dimension primarily arise from collapse of the matrix, electrical leaks from poorly sealed spacers, and uneven heating of the slab gel. I have found that mapping a high-resolution gel image onto convex and concave surfaces provides excellent emulations of the most common types of gel distortion. The resulting images have "pincushion" and "barrel" distortions. The matching algorithm is evaluated by matching the undistorted gel image with the two distorted gels. The results of such an analysis, utilizing the Bio Image software, are shown in Table 1.

7.2. Matching sets of gels

The simplest strategy for matching sets of gel images is to perform numerous pairwise matches. Bio Image and GELLAB-II use this strategy, having all gels matched to a specific reference gel. With the Bio Image system, the reference image can be any gel in the database or a composite gel that has been created by merging several real gels into an artificial image. A variety of other strategies have been employed for the creation of gel databases, many avoiding the use of a single reference gel [54]. QUEST, for example, matches sets of gel images into groups, referred to as matchsets [8]. Each experiment has a matchset created for it and two different experiments are linked together by gel images from samples common to both experiments. Recently, Bio Image also introduced a new matching strategy based upon match sets.

7.2.1. Head-to-head comparison

A comparison between the spot matching capabilities of GELLAB II and Bio Image was recently reported [70]. Both systems require the investigator to select landmarks (anchors) to aid in gel matching. While the Bio Image system allows the user to select different landmarks for each gel pair matched, the GELLAB system requires that the same landmarks be used in all gels matched in the database. GELLAB-II allows the use of 52 while Bio Image permits the use of at least 100 landmarks. GELLAB-II assigns all spots identification numbers regardless of match status. A significant problem encountered with the Bio Image software was that spots not present in the reference gel, were not assigned match identification numbers and were thus not subsequently analyzed. This problem has recently been corrected in the newest version of Bio Image software. Each spot is given a spot number that uniquely defines it within the image. After matching, each spot is given a match number regardless of its match status. The GELLAB-II system lacks the capability for manual interactive editing of spot boundaries and spot matches. Unlike with the Bio Image system, mismatched spots cannot be edited to correct the GELLAB-II database. Additionally, the newest version of Bio Image permits the user to view and edit multiple gel images at a time. This significantly reduces the time required for matching gels.

The estimated labor cost of analyzing 2D gels with the Bio Image and GELLAB-II systems was also evaluated [70]. The investigators estimated that it required approximately six times as much effort to create a Bio Image database relative to a GELLAB-II database. Again, it

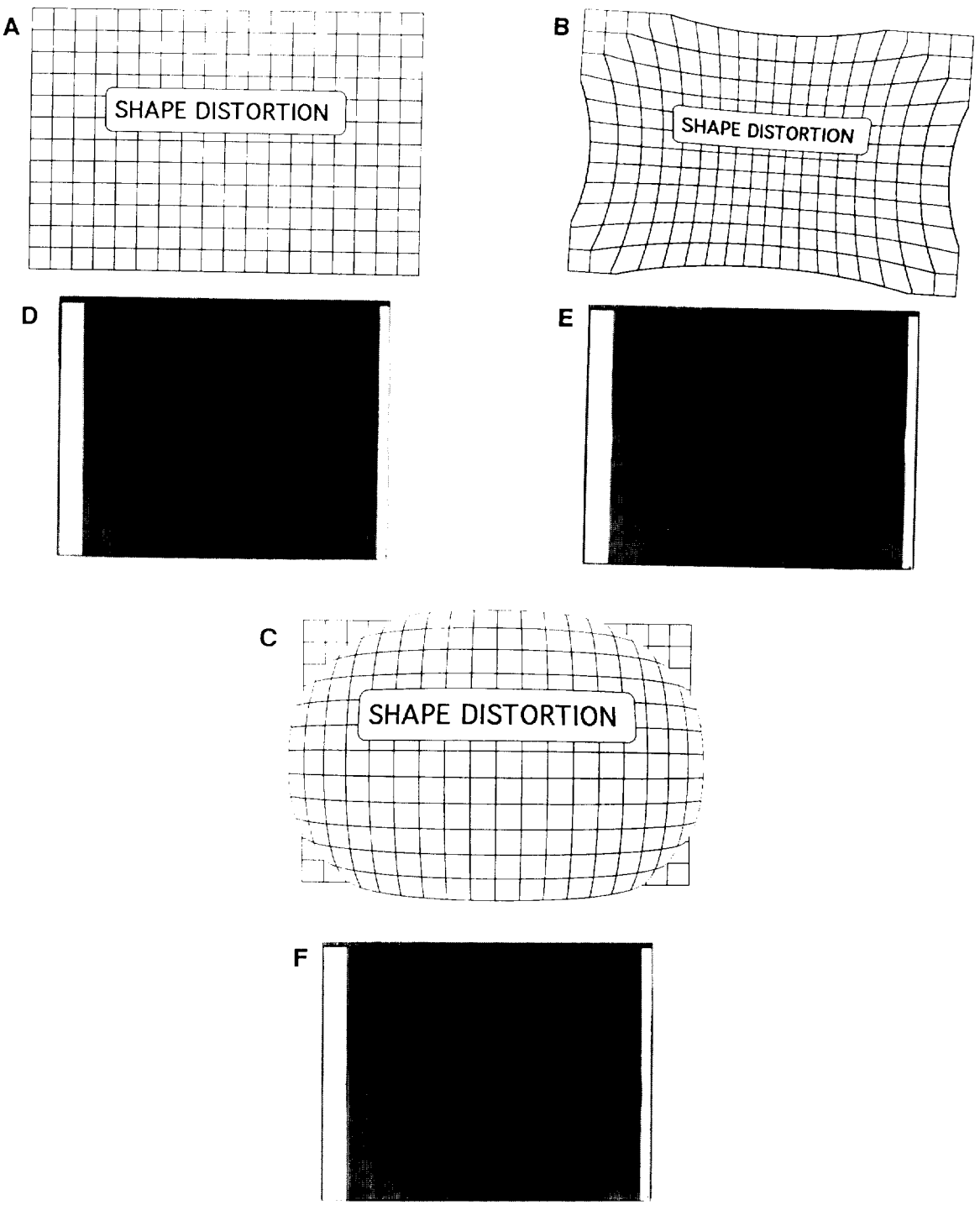

Fig. 9. Introduction of distortions into 2D gels for evaluation of automatic spot matching algorithms. Adobe Photoshop's spherize filter was utilized with amount set to either +50 or −50. (A, D) A rectangular network and standard 2D gel. (B, E) Same images after introduction of a "pincushion" distortion. (C, F) Same images after introduction of a "barrel" distortion. An analysis of the Bio Image gel matching algorithm utilizing the gel images shown in this figure is presented in Table 1.

Table 1
Performance benchmarks: gel matching

Gel	No. of spots detected	% detected	
Control gel	1444	100	
Barrel distortion	1798	124.5	
Pincushion distortion	1860	128.8	
Matches	**No. of matched spots**	**Matchpoints required**	**% matched**
Control to control	1395	3 (computer generated 17 more)	96.6
Control to barrel	1199	45	83.0
Control to pincushion	1216	38	84.2
Control, barrel, pincushion	1059	38–45	75.3

Conclusion: Undistorted gels require 0.21 to 1.3% of the spots to be specified for good matching of the remainder. Highly distorted gels require 2.6 to 3.1% of the spots to be specified for good matching of the remainder.

should be noted that urinary protein profiles are unusual in that they contain a relatively high number of large, saturated spots that require extensive editing by the Bio Image software. Typically, with a complex cell lysate such as endothelial cell proteins, only the actin and vimentin isoforms require manual editing. Recent improvements in the Bio Image software significantly reduce the labor intensiveness of creating a database.

7.2.2. Database queries

High end image analysis systems are capable of simultaneously comparing a large number of 2D gels (10–100), each containing as many as 2000–4000 proteins. The 30 000–50 000 total proteins generated in a typical medium-sized gel database, each have a variety of parameters associated with them. Proteins of interest are automatically identified with user specified queries that are based upon the spot parameters in the database. Ranges of pI, M_r and IA values can be defined. Spot shape quality, spot reproducibility, and minimum magnitude of changes between control and treatment groups can also be specified. A useful query strategy that I often use is: "Find polypeptides reproducibly expressed in the treatment group that differ by two-fold or more from those reproducibly expressed in the control group, that also have integrated A values greater than 0.1, good spot shape quality, M_r values in the range of 20 000 to 150 000 and pI values in the pH range of 4.5 to 7.0". This strategy eliminates irreproducible, very faint, and poor-quality spots from the analysis and identifies changes of a sufficiently large magnitude to be considered biologically relevant.

Much effort is being expended on heuristic clustering techniques for the automatic grouping of similar electrophoretic patterns. Clearly, these methods will have value in certain circumstances, particularly in "cell taxonomy" projects, where the goal may be, for instance, to determine whether a particular tumor cell type is more closely related to a smooth muscle cell or a fibroblast. For most database studies, the investigator knows which gels belong to which category and is willing to share that information with the computer during the set up of the database and subsequent analysis of the information.

8. Ancillary capabilities of imaging systems

8.1. Data interpretation and presentation (statistical analysis and image annotation)

Statistical analysis has been successfully utilized as a method of exploratory analysis to screen large numbers of polypeptides for changes arising from occupational exposure to toxic met-

als [91]. Some image analysis programs provide statistical analysis capabilities for determining whether or not detected changes in polypeptide expression are significant. Generally, some type of Student's *t*-test or ratio tests are utilized. Other packages provide graphics annotation capabilities for presenting gels in publications. I suppose one could argue that the image analysis software should also have word processing capabilities, complete with grammar and spelling checker, so that, after gels are analyzed and figures are generated, one could then write the manuscript. Possibly, the capability to perform on-line literature searches, the capability to organize relevant literature references in a database and an electronic Rolodex for keeping track of phone numbers of important collaborators would be required as well. Unfortunately, many developers of image analysis software have detoured down this road of inane embellishments, rather than addressing the real issues of gel image analysis. Image analysis software packages that do not have every conceivable capability required by the investigator usually permit images and data to be exported to commercial programs that have been developed specifically to address these requirements.

8.2. Image integrity

With a microcomputer and an inexpensive commercial or public domain software package, almost anyone can manipulate images in virtually undetectable ways [92,93]. Needless to say, there is real potential for misuse of these capabilities. As is true in the darkroom, the computer can be used to misleadingly "enrich" bands to support preconceived conclusions. Less ominous scenarios are also foreseeable, where inappropriate algorithms are unwittingly applied to quantitative data, generating spurious results. This is of concern to some scientists, journal editors, and officials of federal agencies, such as the US Food and Drug Administration (FDA). There is concern that the temptation to adjust images to fit hypotheses will be too great for some. Electrophoresis bands can be added or subtracted at will. Contrast can be selectively altered in one region of a gel while leaving others untouched. It is becoming increasingly necessary to set up safeguards against digital fraud. Acceptable boundaries between removing noise from images and using the technology to deliberately deceive need to be clearly delineated. Some possible safeguards could include the requirement that researchers preserve an electronic history of an image, including all changes made to it, and that papers alert readers to the use of the technology to generate the image.

A similar problem arose in chromatography several years ago. Traditionally chromatograms were generated on paper by a strip chart recorder, but since the 1980s most have been generated digitally in computers. In 1991, the FDA established the Good Automated Laboratory Practices (GALP) guidelines, requiring that laboratories archive the original, unedited data display and a trail of any changes made. It appears that the best solution to the problem would be that the electrophoretic imaging system itself would create tamperproof records of the original data [94]. Several possible implementations of this concept are being considered. The camera system could generate a proprietary image in a write-once-read-many-times (WORM) format, allowing the user to then copy the image and make modifications. Alternatively, a digital signature of the original data could be permanently appended to an image that allows the resurrection of the original data by anyone needing to verify its authenticity.

8.3. Virtual laboratories

The concept of a worldwide system of interconnected computer networks (information super highways) heralding a new age of "electronic communities" has become popularized in the press in recent years [95,96]. "Virtual laboratories" are envisioned consisting of collections of researchers in a common field linked electronically and having the ability to share information, instruments, software and computing capability [95,96]. Such video conferencing

has been popular in the high-energy physics community for several years [97].

Some strides have been made towards the development of gel image teleconferencing capabilities [98]. The primary goal of one such implementation, Xconf, is to share and interactively discuss textual and image data between multiple remote computer displays in real-time [98]. Xconf is implemented using existing national and international networks (the Internet) and the network-based M.I.T. X-Window System graphics displays [98]. Only one site participating in the conference is required to have the Xconf software. Data are transparently passed by X-Windows from one system to another using standard TCP/IP or DECnet protocols. Remotely located collaborators can be simultaneously connected to the same 2D gel database for interactive "brainstorming" and data exploration.

Telephone conferencing, Faxes and electronic mail (E-mail) are considered by the proponents of the new technology to be less spontaneous, dynamic and immediate than multimedia computer-conferencing. Without standardization of electrophoretic methods, it is doubtful that many investigators will have a pressing need for elaborate video-conferencing capabilities. I have found that overnight mail, telephones and Faxes fully meet all my present collaborative needs. If one considers that it may require a month or more to perform an experiment from raw sample through gel databasing, overnight mail is incredibly fast.

9. Performance criteria; institutional facility perspective

As should be obvious from the previous sections, the field of quantitative 2D gel analysis is conspicuous in its lack of standardization of approach, in terms of both data acquisition and data analysis. This should not be surprising since there is no consensus with respect to the electrophoretic separation itself either. The length of the IEF gel and the width and height of the second-dimension SDS-PAGE gel may differ by as much as a factor of five between different laboratories. Even when presenting electrophoretic patterns in journals, authors are as likely to have the acidic region to the left as they are to have the basic region to the left.

A fairly sophisticated analysis system is required to construct a high-resolution 2D gel database. The system must minimally provide information about the protein's M_r, pI and quantity. It is readily apparent that the systems developed by various laboratories differ with respect to the method of obtaining the three physical parameters necessary for the protein database. It is not obvious, however, whether a second-derivative or first-derivative analysis is best for identifying spot boundaries, whether utilizing non-parametric or parametric spot finding methods will substantially influence the outcome of an analysis, or whether convolution filtering or repetitive scanning is most suitable for noise elimination. Procedures for the quantitative analysis of 2D gels differ greatly in terms of labor intensiveness, sensitivity, complexity, and cost. When developing a quantitative image analysis facility, it is necessary to minimize labor intensiveness, and maximize the sensitivity of the instrument within the monetary constraints of the laboratory. The complexity of the analysis is often dictated by the requirements of the research project.

It is impossible to recommend a specific image acquisition device or computerized image analysis system that meets the needs of every investigator and every core facility. Some full-featured image analysis workstations cost in the neighborhood of US$ 100 000 [93]. It is also feasible to utilize public domain software, a microcomputer and an inexpensive document scanner to perform many basic image analysis tasks for less than US$ 1500. A signal transduction laboratory may require phosphor storage or multichannel plate analyzers for high-throughput analysis of phosphoproteins. Heuristic clustering may be critically important to a microbiology laboratory involved in classifying organisms. Another laboratory may only require that a few spots be quantified by manual assignment of spot borders, thus obviated the need for expensive high-end image analysis systems.

In order to satisfy the needs of a large number

of scientists, an institutional core facility requires a fairly sophisticated computerized image analysis workstation, capable of automatic gel matching, and image databasing. If the facility only has funds for a single image acquisition device, then a CCD camera-based system is most appropriate, since it can be utilized for the widest variety of samples. Additionally, a laser printer for generating reports and a color printer for generating poster and publication quality prints is very valuable. Finally, a cross-platform network is useful for allowing the export of image and data files to microcomputers for further analysis and annotation.

10. Conclusions

The field of computer-assisted gel image analysis is rapidly advancing. Many of the public domain and commercial systems are still undergoing rapid development and continual modification. Few direct comparisons among different systems have been performed due to the inherent complexity and expensiveness of the instruments. The comparisons that have been performed are usually out of date before appearing in the literature, due to upgraded capabilities added to the software and advancements in computer technology. From personal experience, I have found that a state-of-the-art image analysis facility established today, will only be an average one in three years time. When establishing an image analysis facility it is best to evaluate the requirements of the investigators who will utilize it and attempt to anticipate their needs over the next five years. A system that barely meets the current needs of its clients will quickly become a source of much frustration to them. Finally, it is important to remember that the performance of an image analysis system can be greatly improved by providing it with optimized electrophoretic patterns, free of defects.

References

[1] Y. Aloimonos and A. Rosenfeld, *Science*, 253 (1991) 1249.
[2] E. Adelson, *Science*, 262 (1993) 2042.
[3] P. Lemkin, C. Merril, L. Lipkin, M. Van Keuren, W. Oertel, B. Shapiro, M. Wade, M. Schultz and E. Smith, *Comput. Biomed. Res.*, 12 (1979) 517.
[4] S. Spragg, M. Jones and B. Hill, *Anal. Biochem.*, 129 (1983) 255.
[5] R. Hampton and S. Rutam, *Anal. Chem.*, 65 (1993) 894.
[6] H. van Lith, M. Haller, L. van Zutphen and A. Beynen, *Anal. Biochem.*, 201 (1992) 288.
[7] D. Kleiner and W. Stetler-Stevenson, *Anal. Biochem.*, 218 (1994) 325.
[8] J. Garrels and B. Franza, *J. Biol. Chem.*, 264 (1989) 5283.
[9] J. Garrels and B. Franza, *J. Biol. Chem.*, 264 (1989) 5299.
[10] J. Celis and E. Olsen, *Electrophoresis*, 15 (1994) 309.
[11] J. Hunter and S. Hunter, *Anal. Biochem.*, 164 (1987) 430.
[12] W. Patton, L. Lam, Q. Su, M. Lui, H. Erdjument-Bromage and P. Tempst, *Anal. Biochem.*, 220 (1994) 324
[13] S. Clark, in J.C. Venter and L.C. Harrison (Editors), *Receptor Purification Procedures* Alan R. Liss, New York, 1984, p. 149.
[14] R. Appel, D. Hochstrasser, M. Funk, C. Pellegrini, A. Muller and J. Scherrer, *Electrophoresis*, 12 (1991) 722.
[15] R. Appel, G. Bologna and D. Hochstrasser, in A. Reichert, B. Sadan, S. Bengtsson, J. Bryant and U. Piccolo (Editors), *Proceedings of MIE 93*, Freund Publ. House, London, 1993, p. 40.
[16] D. Hochstrasser and J. Tissot, *Adv. Electrophoresis*, 6 (1993) 270.
[17] J. Myrick, S. Caudill, M. Robinson and I. Hubert, *Appl. Theor. Electrophoresis*, 3 (1993) 137.
[18] W. Patton, M. Yoon, J. Alexander, N. Chung-Welch, H. Hechtman and D. Shepro, *J. Cell. Physiol.*, 143 (1990) 140.
[19] N. Chung-Welch, W. Patton, G. Yen-Patton, H. Hechtman and D. Shepro, *Differentiation*, 42 (1989) 44.
[20] W. Patton, M. Pluskal, W. Skea, J. Buecker, M. Lopez, R. Zimmerman, L. Belanger and P. Hatch, *BioTechniques*, 8 (1990) 518.
[21] W. Patton, M. Lopez, P. Barry and W. Skea, *BioTechniques*, 12 (1992) 580.
[22] C. Merril, *Adv. Electrophoresis*, 1 (1987) 111.
[23] T. Rabilloud, *Electrophoresis*, 13 (1992) 429.
[24] L. Rodriguez, D. Gersten, L. Ramagli and D. Johnston, *Electrophoresis*, 14 (1993) 628.
[25] J. Garrels, *J. Biol. Chem.*, 254 (1979) 7961.
[26] D. Rowlands, A. Flook, P. Payne, A. van Hoff, T. Niblett and S. McKee, *Electrophoresis*, 9 (1988) 820.
[27] W. Patton, A. Chen, N. Chung-Welch, R. Cambria, A. Marks, M. Taubman and P. Tempst, *Mol. Biol. Cell.*, 3 (suppl.) (1992) 179a.
[28] W. Patton, H. Erdjument-Bromage, A. Chen, L. Lam, Q. Su, M. Lui, A. Marks, M. Taubman and P. Tempst, in preparation.

[29] J. Celis, H. Rasmussen, E. Olsen, P. Madsen, H. Leffers, B. Honore, K. Dejgaard, P. Gromov, H. Hoffman, M. Nielsen, A. Vassilev, O. Vintermyr, J. Hao, A. Celis, B. Basse, J. Lauridsen, G. Ratz, A. Andersen, E. Walbum, I. Kjaergaard, M. Puype, J. Van Damme and J. Vandekerckhove, *Electrophoresis*, 14 (1993) 1091.
[30] C. Shanahan, P. Weissberg and J. Metcalfe, *Circ. Res.*, 73 (1993) 193.
[31] C. Bordier, *J. Biol. Chem.*, 256 (1981) 1604.
[32] M. Ramsby, G. Makowski and E. Khairallah, *Electrophoresis*, 15 (1994) 265.
[33] P. Jungblut, H. Baumeister and J. Klose, *Electrophoresis*, 14 (1993) 638.
[34] P. Jungblut and J. Klose, *J. Chromatogr.*, 482 (1989) 125.
[35] L. Miribel, E. Gianazza and P. Arnaud, *J. Biochem. Biophys. Methods*, 16 (1988) 1.
[36] W. Quitsche and N. Schechter, *Anal. Biochem.*, 124 (1982) 231.
[37] J. Sutherland, *Adv. Electrophoresis*, 6 (1993) 1.
[38] C. Watkins, A. Sadun and S. Marenka, *Modern Image Processing; Warping, Morphing, and Classical Techniques*, Academic Press, New York, 1993.
[39] *Image Analysis: Principles and Practice; Joyce-Loebl Technical Handbook*, Short Run Press, Exeter, 1985, p.87.
[40] P. Lemkin, J. Myrick and K. Upton, *Appl. Theor. Electrophoresis*, 3 (1993) 163.
[41] R. Johnston, S. Pickett and D. Barker, *Electrophoresis*, 11 (1990) 355.
[42] Y. Amemiya and J. Miyahara, *Nature*, 336 (1988) 89.
[43] S. Patterson and G. Latter, *BioTechniques*, 15 (1993) 1076.
[44] R. Templer, *Nucl. Instr. Meth. Phys. Res. (A)*, 300 (1991) 357.
[45] W. Reichert, J. Stein, B. French, P. Goodwin and U. Varanasi, *Carcinogenesis*, 13 (1992) 1475.
[46] R. Johnston, S. Pickett and D. Barker, *Methods: Companion Methods Enzymol.*, 3 (1991) 128.
[47] M. Harrington, L. Hood and C. Puckett, *Methods: Companion Methods Enzymol.*, 3 (1991) 135.
[48] M. Ross, G. Latter, S. Burbeck and J. Leavitt, *Electrophoresis*, 8 (1987) 249.
[49] D. Englert, N. Roessler, A. Jeavons and S. Fairless, *Cell. Mol. Biol.*, (1994) in press.
[50] D. Sullivan, P. Auron, G. Quigley, P. Watkins, J. Stanchfield and C. Bolon, *BioTechniques*, 5 (1987) 672.
[51] A. Jeavons, *US Pat.*, 5 138 168 (1992).
[52] H. Yamamoto, M. Nakatani, K. Shinya, B. Kim and T. Kakuno, *Anal. Biochem.*, 191 (1990) 58.
[53] M. Lanan, D. Grossman and M. Morris, *Electrophoresis*, 15 (1994) 137.
[54] M. Miller, *Adv. Electrophoresis*, 3 (1989) 181.
[55] P. Vincens, N. Paris, J. Pujol, C. Gaboriaud, T. Rabilloud, J. Pennetier, P. Matherat and P. Tarroux, *Electrophoresis*, 7 (1986) 347.
[56] L. Lipkin and P. Lemkin, *Clin. Chem.*, 26 (1980) 1403.
[57] P. Lemkin and L. Lipkin, *Comput. Biomed. Res.*, 14 (1981) 272.
[58] W. Patton and P. Tempst, *Electrophoresis*, 14 (1993) 650.
[59] C. Mariash, S. Seelig and S. Oppenheimer, *Anal. Biochem.*, 121 (1982) 386.
[60] W. Patton, M. Dhanak and B. Jacobson, *Anal. Biochem.*, 179 (1989) 37.
[61] C. Lindley, *Practical Image Processing in C; Acquisition, Manipulation, Storage*, Wiley, New York, 1991, p. 347.
[62] P. Lennard, *Nature*, 347 (1990) 103.
[63] P. Rogan, P. Lemkin and A. Klar, *Methods: Companion Methods Enzymol.*, 3 (1991) 91.
[64] U. Romling and B. Tummler, *Electrophoresis*, 14 (1993) 283.
[65] P. Lemkin and P. Rogan, *Appl. Theor. Electrophoresis*, 2 (1991) 141.
[66] N. McFerran and T. Quigley, *Biochem. Soc. Trans.*, 12 (1984) 1000.
[67] J. Bossinger, M. Miller, K. Vo, E. Geiduschek and N. Xuong, *J. Biol. Chem.*, 254 (1979) 7986.
[68] M. Miller and C. Merril, *Appl. Theor. Electrophoresis*, 1 (1989) 127.
[69] J. Vohradsky and J. Panek, *Electrophoresis*, 14 (1993) 601.
[70] J. Myrick, P. Lemkin, M. Robinson and K. Upton, *Appl. Theor. Electrophoresis*, 3 (1993) 335.
[71] Y. Wu, P. Lemkin and K. Upton, *Electrophoresis*, 14 (1993) 1351.
[72] J. Solomon and M. Harrington, *Comput. Appl. Biosci.*, 9 (1993) 133.
[73] K. Oerter, P. Munson, W. McBride and D.Rodbard, *Anal. Biochem.*, 189 (1990) 235.
[74] D. Rodbard, *Clin. Chem.*, 20 (1974) 1255.
[75] G. Cantu and J. Nelson, *BioTechniques*, 16 (1994) 322.
[76] B.Hammes, in B. Hammes and D. Rickwood (Editors), *Gel Electrophoresis of Proteins: A Practical Approach*, IRL Press, Oxford, Washington, DC, 1981, p. 15.
[77] X. Gitton, G. Andre-Fontaine, F. Andre and J. Ganiere, *Vet. Microbiol.*, 32 (1992) 293.
[78] V. Winston, *Electrophoresis*, 10 (1989) 220.
[79] W. Patton, N. Chung-Welch, M. Lopez, R. Cambria, B. Utterback and W. Skea, *Anal. Biochem.*, 197 (1991) 25.
[80] M. Butterman, D.Tietz, L. Orban and A. Chrambach, *Electrophoresis*, 9 (1988) 293.
[81] K. Ferguson, *Metabolism*, 13 (1964) 985.
[82] P.Righetti, *Isoelectric Focusing: Theory, Methodology and Applications (Laboratory Techniques in Biochemistry and Molecular Biology*, Vol. 11) Elvesier, Amsterdam, New York, 1983, p. 299.
[83] N. Anderson and B. Hickman, *Anal. Biochem.*, 93 (1979) 312.
[84] B. Bjellqvist, B. Basse, E. Olsen and J.Celis, *Electrophoresis*, 15 (1994) 529.
[85] D. Dean, M. Cronan, J. Gardner, P. Connelly and J. Celis, *Electrophoresis*, 15 (1994) 540.

[86] M. Miller, A. Olson and S. Thorgeirsson, *Electrophoresis*, 5 (1984) 297.
[87] K. Conradsen and J. Pedersen, *Biometrics*, 48 (1992) 1273.
[88] M. Starita-Geribaldi, A. Houri and P. Sudaka, *Electrophoresis*, 14 (1993) 773.
[89] J. Sanders, A. Petterson, P. Hughs, C. Connell, M. Raff, S. Menchen, L. Hood and D. Teplow, *Electrophoresis*, 12 (1991) 3.
[90] C. Glasbey and F. Wright, *Electrophoresis*, 15 (1994) 143.
[91] S. Caudill, J. Myrick and M. Robinson, *Appl. Theor. Electrophoresis*, 3 (1993) 133.
[92] C. Anderson, *Science*, 263 (1994) 317.
[93] F. Hoke, *The Scientist*, 21 March (1994) 18.
[94] G. Tanbes, *Science*, 263 (1994) 318.
[95] R. Pool, *Science*, 261 (1993) 841.
[96] W. Wulf, *Science*, 261 (1993) 854.
[97] R. Crease, *Science*, 264 (1994) 654.
[98] P. Lemkin, *Comput. Biomed. Res.*, 26 (1993) 1.